CKDMIP: CKD tool performance evaluation

May 21, 2020

CKD tool: **ecCKD version 0.6**
Spectral domain: **Shortwave**
Application: **Climate**
Evaluation dataset: **Evaluation-1**

Contents

Overview

This automatically generated document contains an evaluation of the performance of ecCKD for generating shortwave correlated k-distribution (CKD) gas-optics models targeting the application *Climate*: atmospheric heating rates are required to a minimum pressure of 0.02 hPa, and evaluation is performed for a wide range of greenhouse gas concentrations. The evaluation dataset is *Evaluation-1* from the Correlated K-Distribution Model Intercomparison Project (CKDMIP)[1]. Shorwave radiative transfer is performed using a two-stream solver. The ecCKD tool has been used to generate CKD models with the following band structure(s): *wide* (5 bands) and *narrow* (13 bands). For each band structure, a number of CKD models have been generated, characterized by the total number of k terms (also known as g points).

[1] `https://confluence.ecmwf.int/display/CKDMIP`

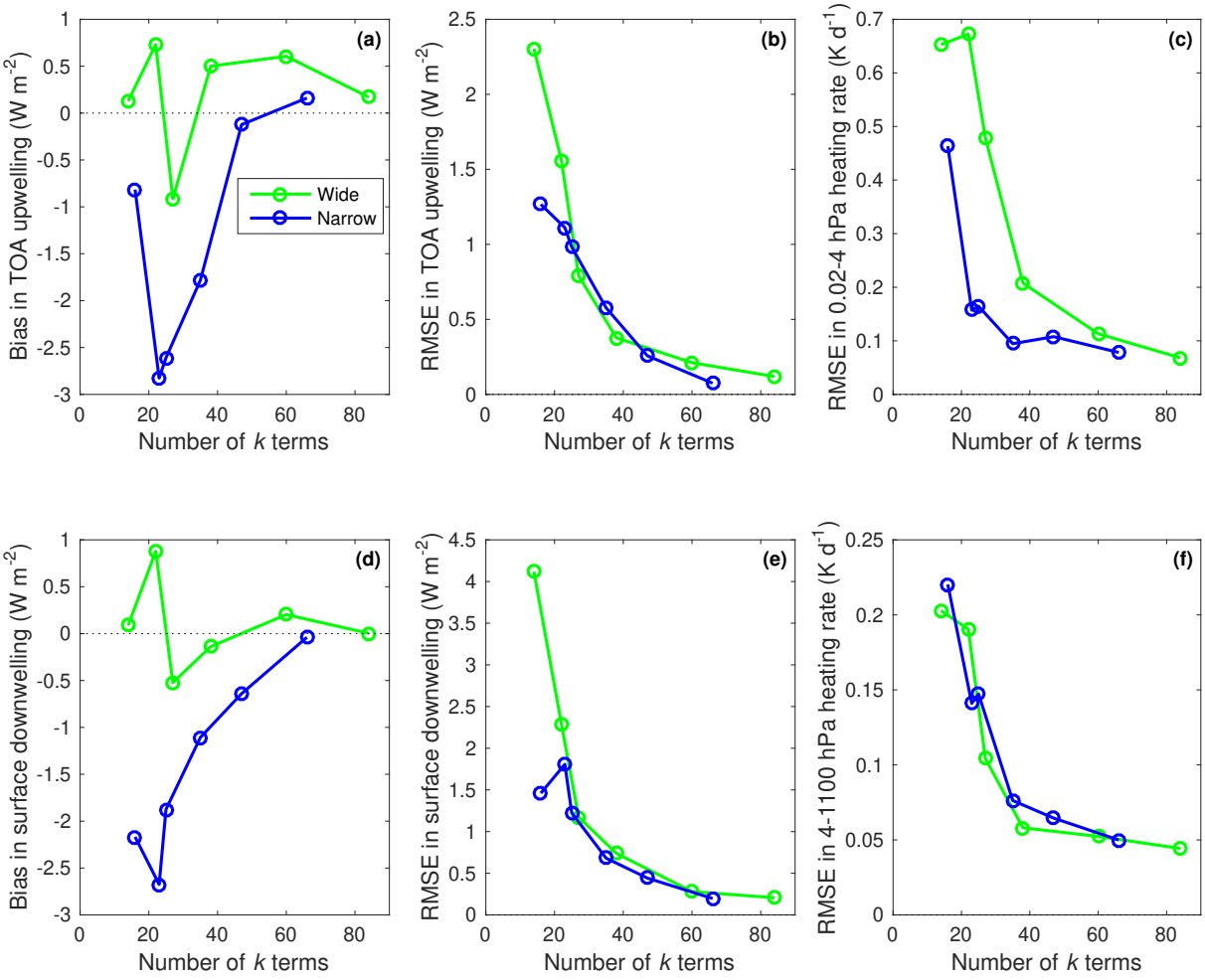

Biases and root-mean-squared errors (RMSE) in top-of-atmosphere (TOA) upwelling irradiance and surface downwelling irradiance, and RMSE in heating rate for two pressure ranges, for the various band structures as a function of the total number of k terms. It was computed from the CKDMIP scenarios 1–18, which cover climate conditions from glacial maximum up to the worst of the CMIP6 future scenarios, and perturbations of the individual greenhouse gases CO_2, CH_4 and N_2O.

Model 1: ecCKD climate-wide-14

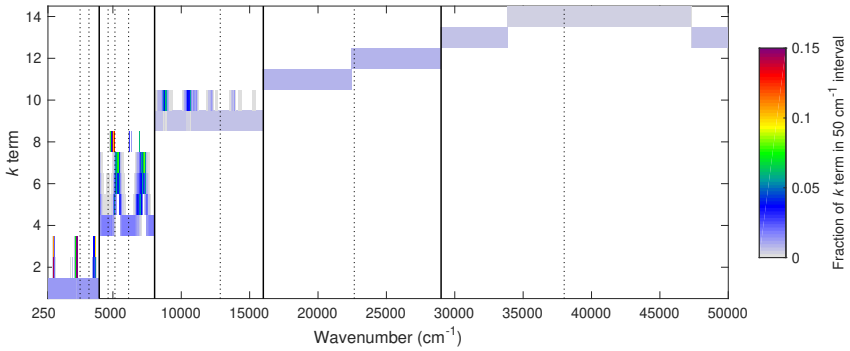

Illustration of the parts of the shortwave spectrum that contribute to each k term of the climate-wide-14 model.

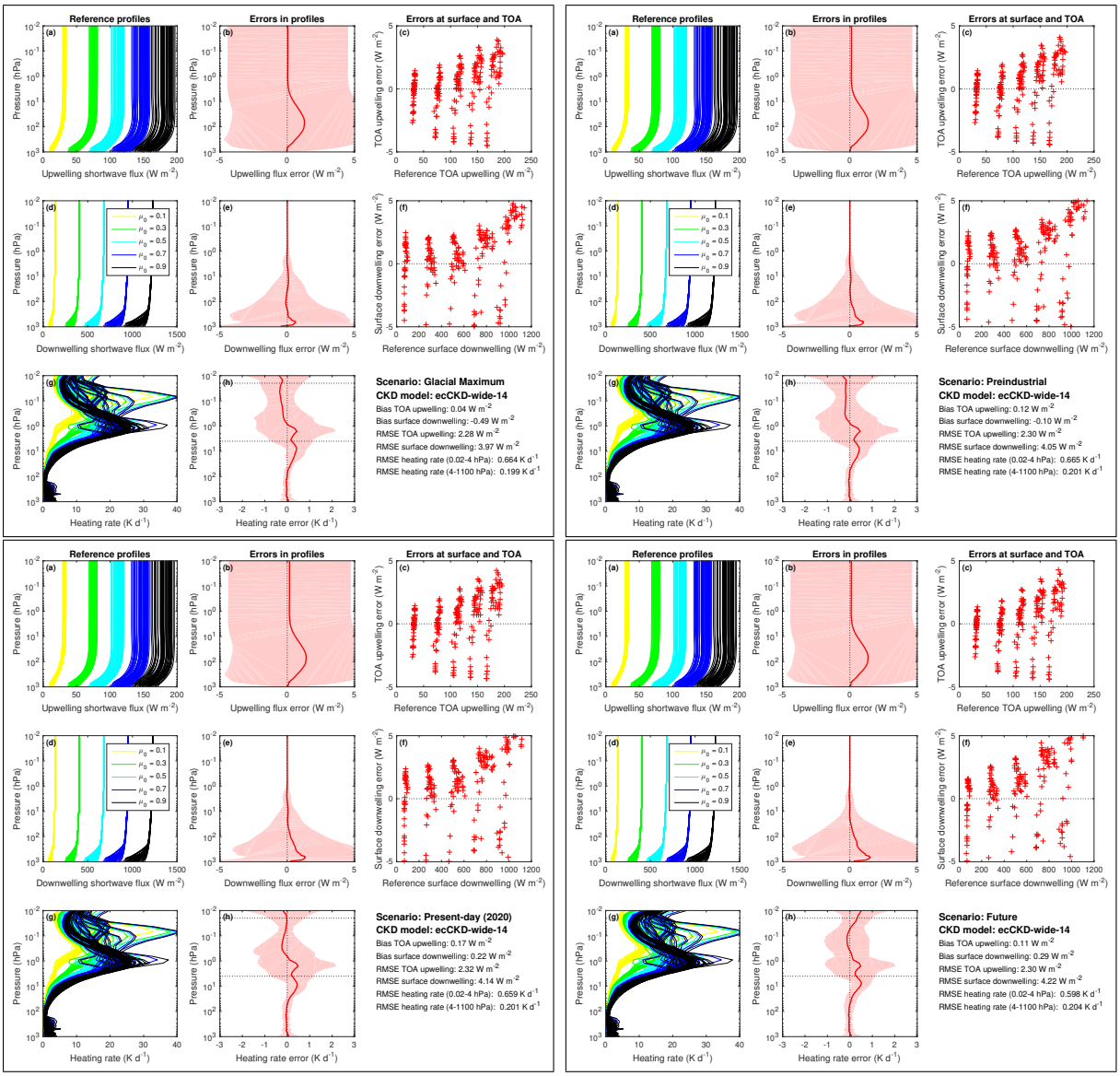

Each boxed group of panels evaluate the climate-wide-14 CKD model for a single CKDMIP scenario. The left three panels in each group show the irradiances and heating rates from the reference line-by-line calculations for five values of the cosine of the solar zenith angle, μ_0. The red lines in the middle three panels show the corresponding bias in these quantities from the CKD model. The shaded regions encompass 95% of the instantaneous errors. Panels c and f depict instantaneous errors in upwelling TOA and downwelling surface irradiances.

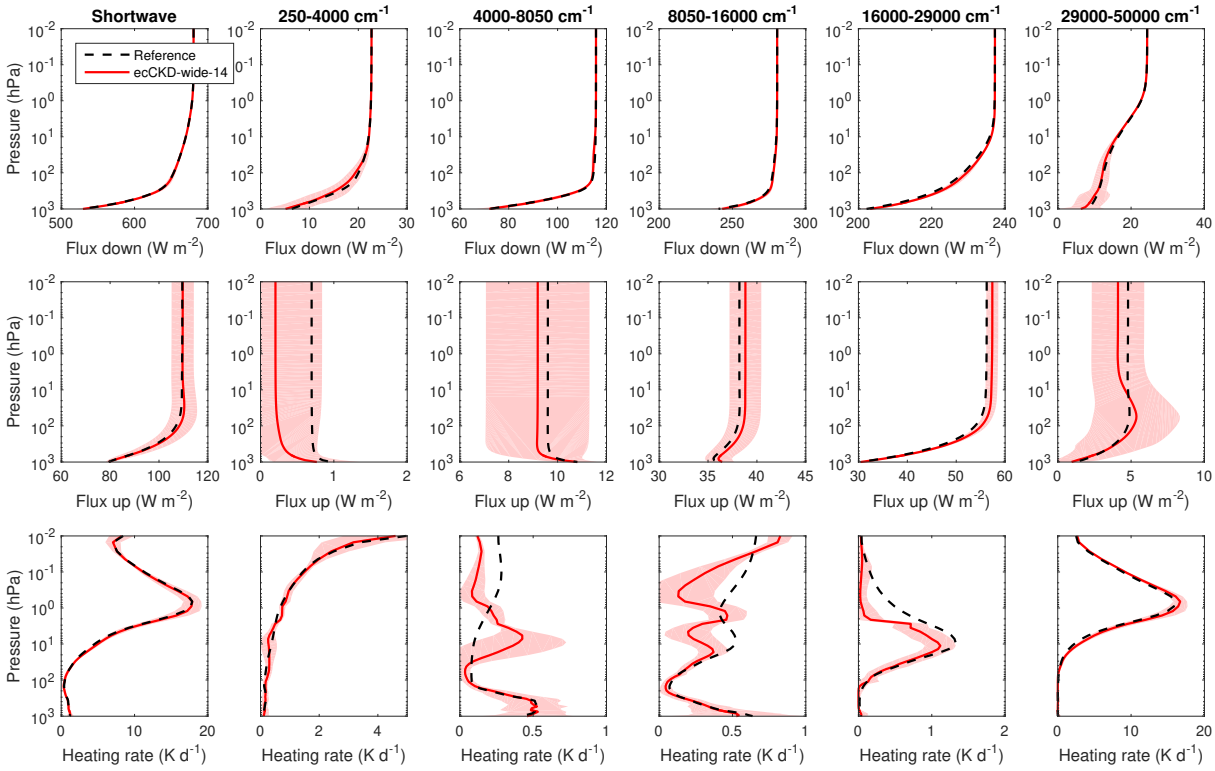

Evaluation of irradiances and heating rates for the broadband (leftmost column of panels) and the 5 wide shortwave bands (other panels) of the climate-wide-14 CKD model. The black dashed and red solid lines correspond to the average of the 50 profiles for the "present-day" scenario, while the shaded regions encompass 95% of the error.

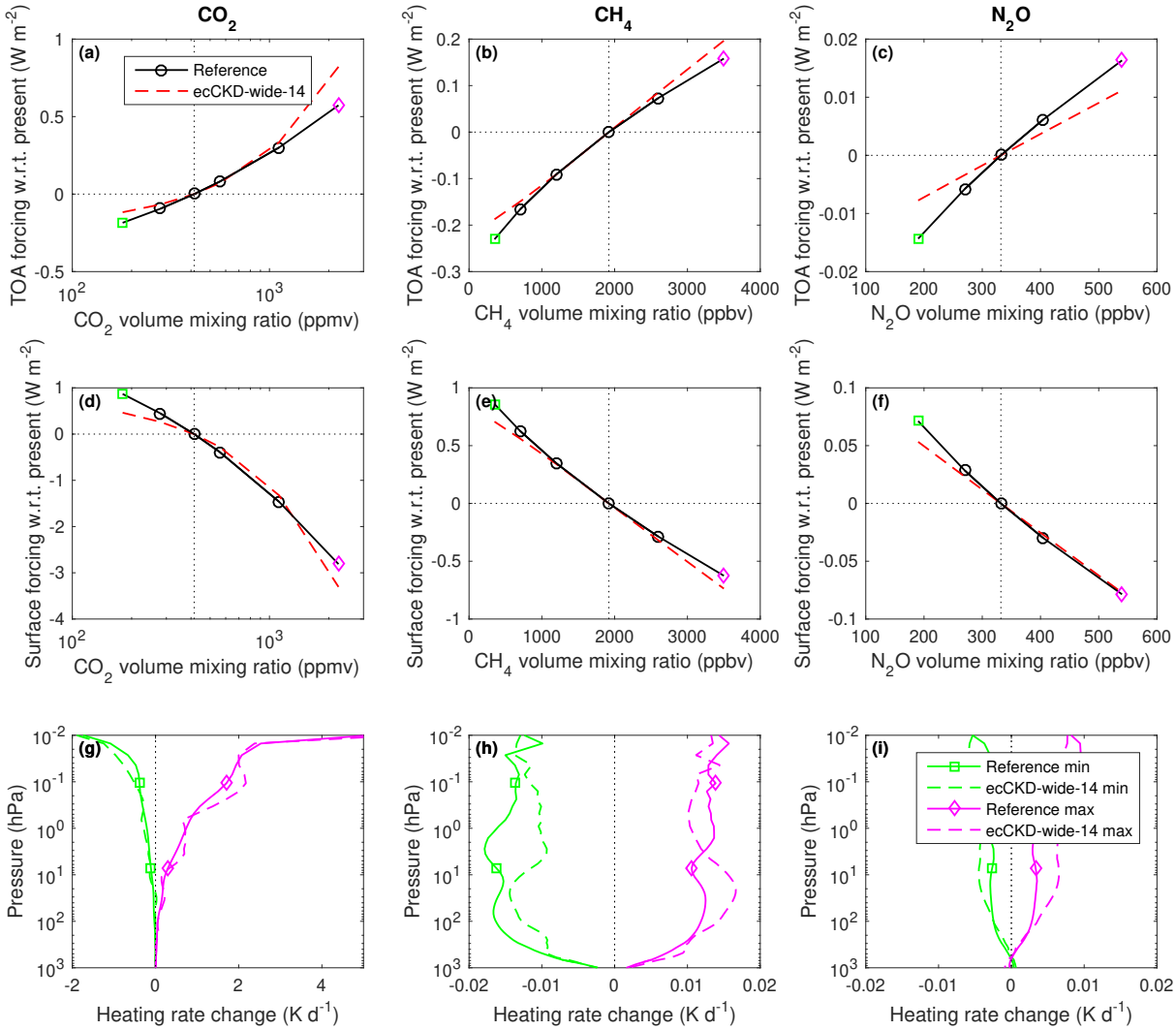

Comparison of reference line-by-line and calculations by the climate-wide-14 model of the instantaneous clear-sky radiative forcing from perturbing each of the five well-mixed greenhouse gases from their present-day values, at (top row) top-of-atmosphere and (middle row) surface, averaged over the 50 profiles of the Evaluation-1 dataset. The bottom row shows the mean change to heating rate resulting from perturbing the concentration of a gas from its present-day value to either the maximum or minimum value in the range for that gas.

Model 2: ecCKD climate-wide-22

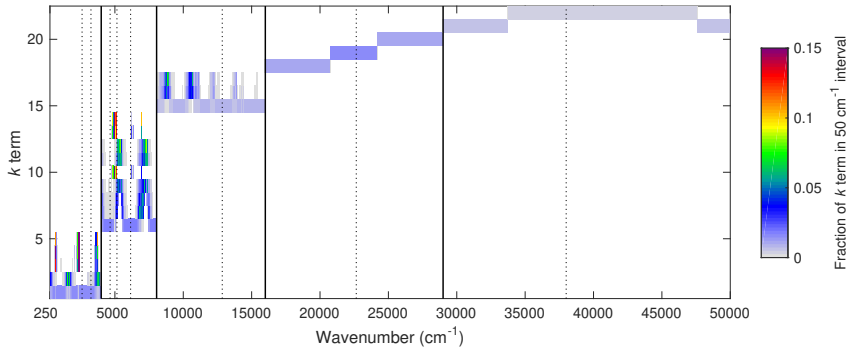

Illustration of the parts of the shortwave spectrum that contribute to each k term of the climate-wide-22 model.

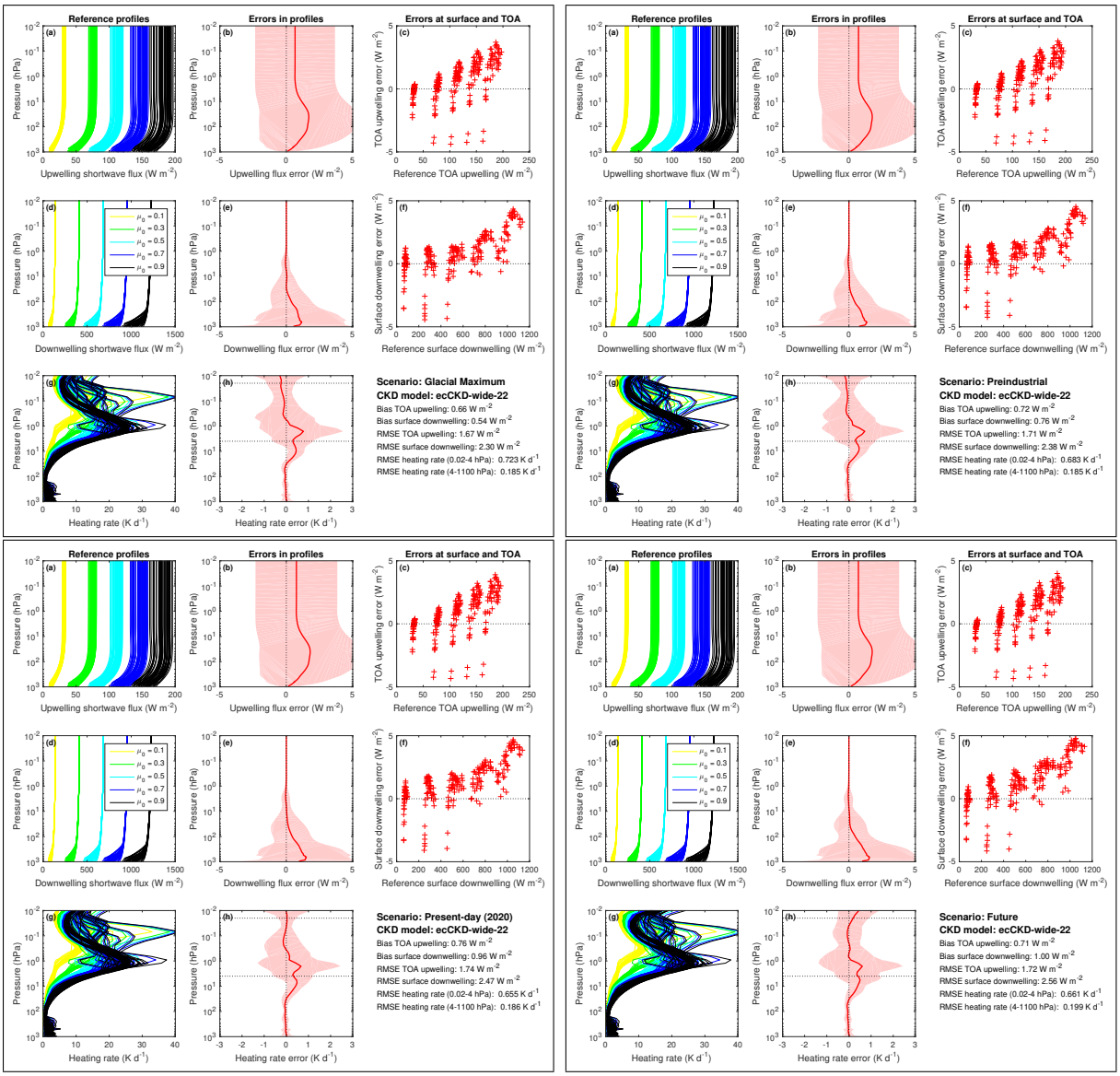

Each boxed group of panels evaluate the climate-wide-22 CKD model for a single CKDMIP scenario. The left three panels in each group show the irradiances and heating rates from the reference line-by-line calculations for five values of the cosine of the solar zenith angle, μ_0. The red lines in the middle three panels show the corresponding bias in these quantities from the CKD model. The shaded regions encompass 95% of the instantaneous errors. Panels c and f depict instantaneous errors in upwelling TOA and downwelling surface irradiances.

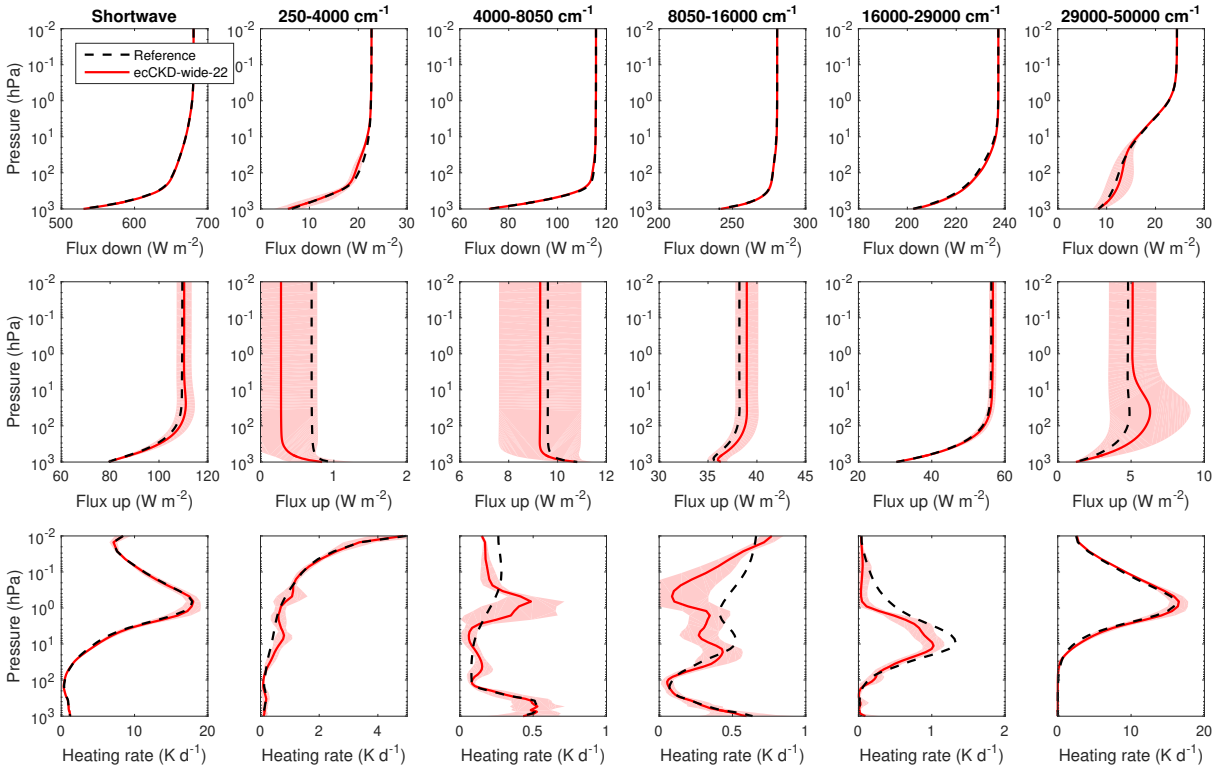

Evaluation of irradiances and heating rates for the broadband (leftmost column of panels) and the 5 wide shortwave bands (other panels) of the climate-wide-22 CKD model. The black dashed and red solid lines correspond to the average of the 50 profiles for the "present-day" scenario, while the shaded regions encompass 95% of the error.

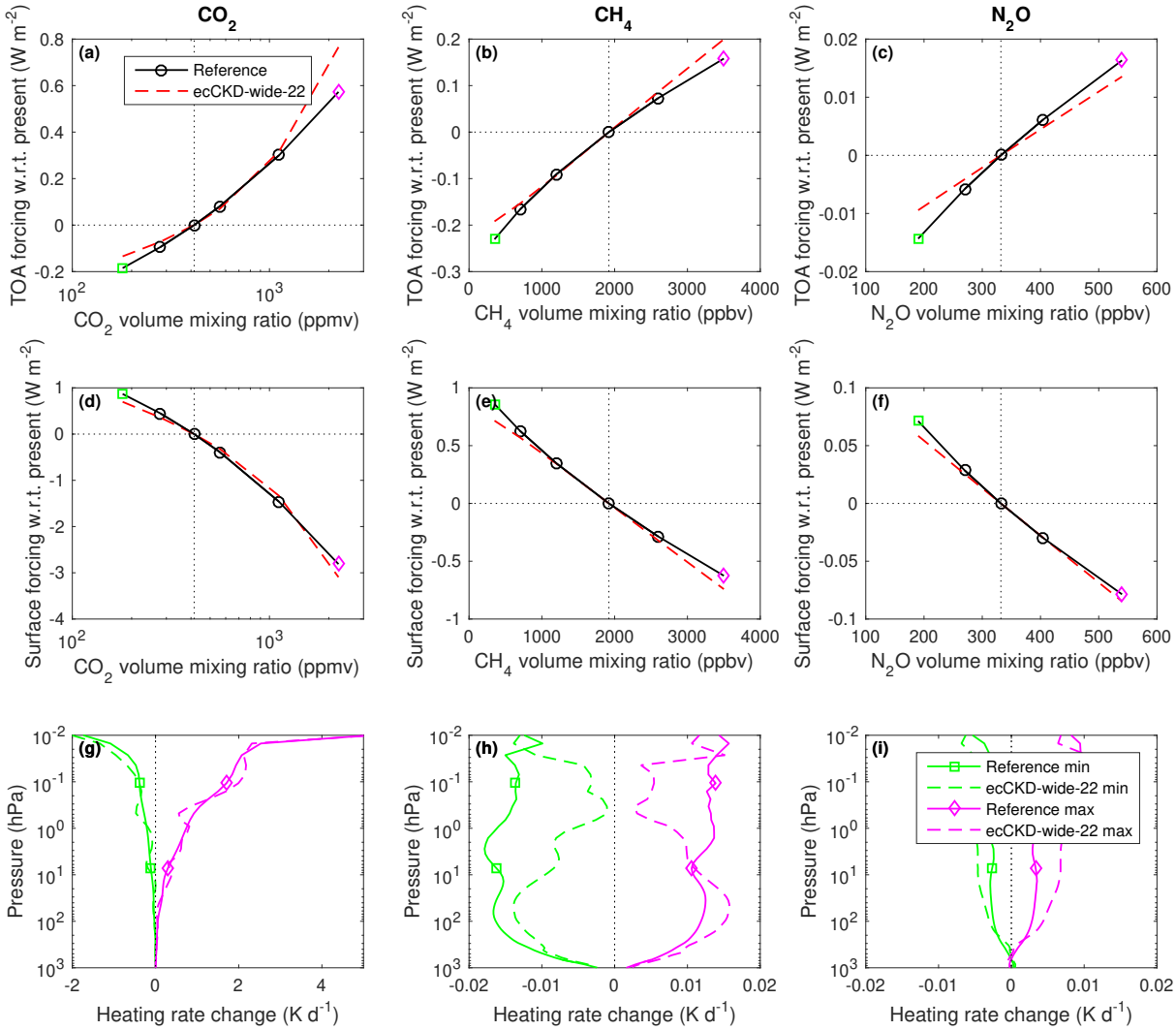

Comparison of reference line-by-line and calculations by the climate-wide-22 model of the instantaneous clear-sky radiative forcing from perturbing each of the five well-mixed greenhouse gases from their present-day values, at (top row) top-of-atmosphere and (middle row) surface, averaged over the 50 profiles of the Evaluation-1 dataset. The bottom row shows the mean change to heating rate resulting from perturbing the concentration of a gas from its present-day value to either the maximum or minimum value in the range for that gas.

Model 3: ecCKD climate-wide-27

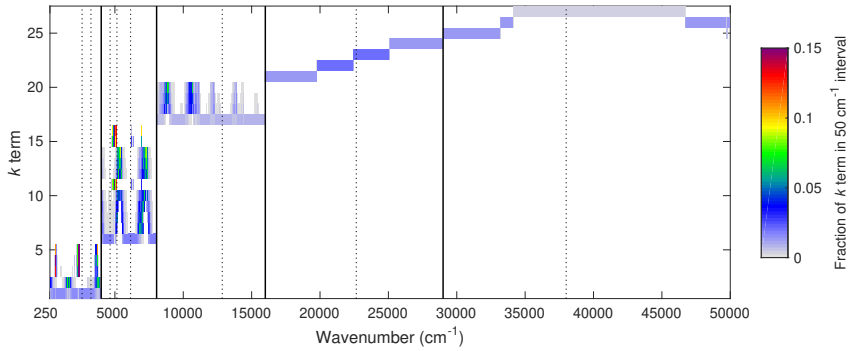

Illustration of the parts of the shortwave spectrum that contribute to each k term of the climate-wide-27 model.

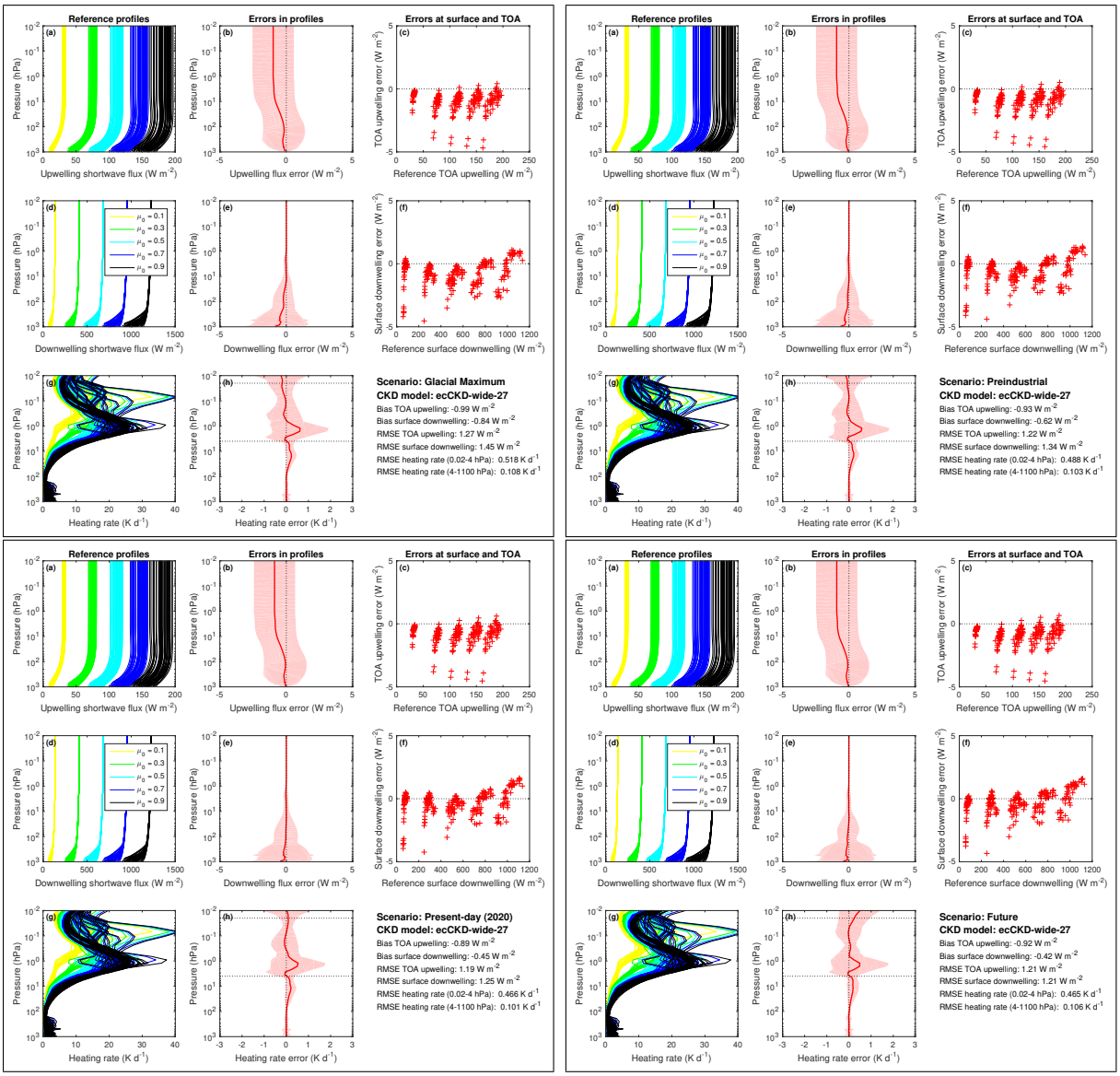

Each boxed group of panels evaluate the climate-wide-27 CKD model for a single CKDMIP scenario. The left three panels in each group show the irradiances and heating rates from the reference line-by-line calculations for five values of the cosine of the solar zenith angle, μ_0. The red lines in the middle three panels show the corresponding bias in these quantities from the CKD model. The shaded regions encompass 95% of the instantaneous errors. Panels c and f depict instantaneous errors in upwelling TOA and downwelling surface irradiances.

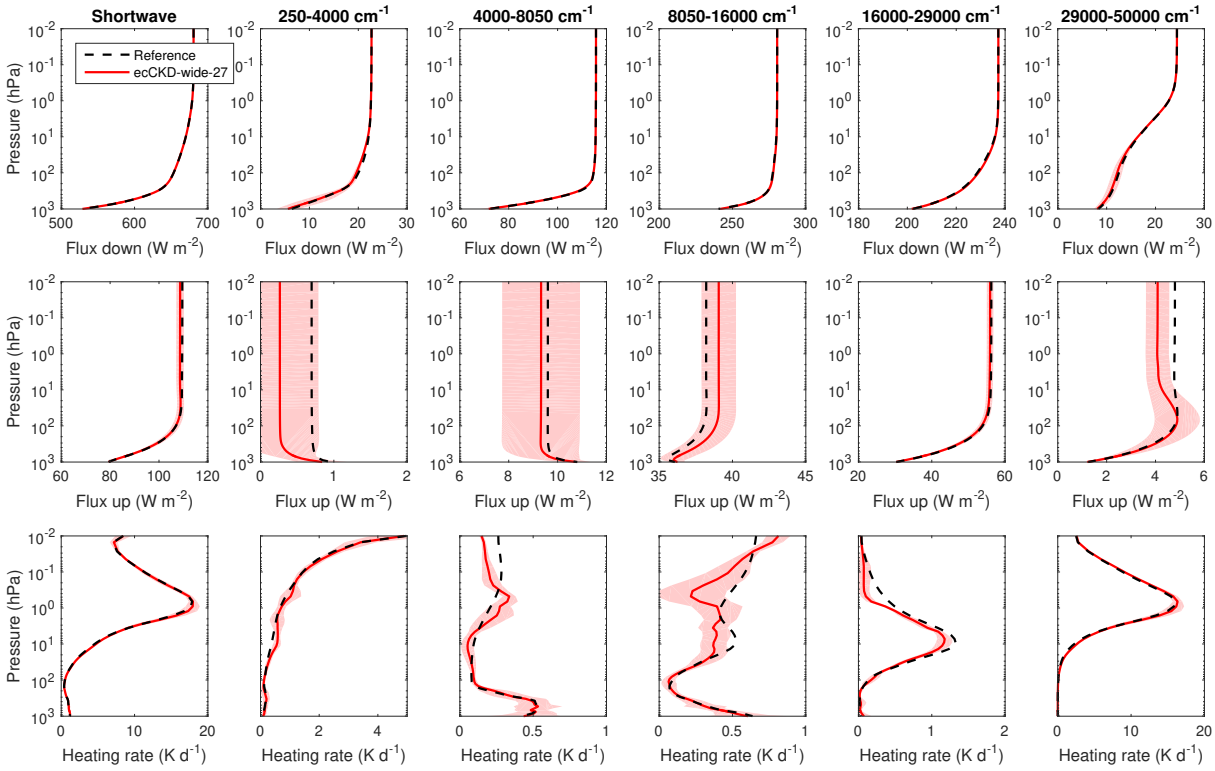

Evaluation of irradiances and heating rates for the broadband (leftmost column of panels) and the 5 wide shortwave bands (other panels) of the climate-wide-27 CKD model. The black dashed and red solid lines correspond to the average of the 50 profiles for the "present-day" scenario, while the shaded regions encompass 95% of the error.

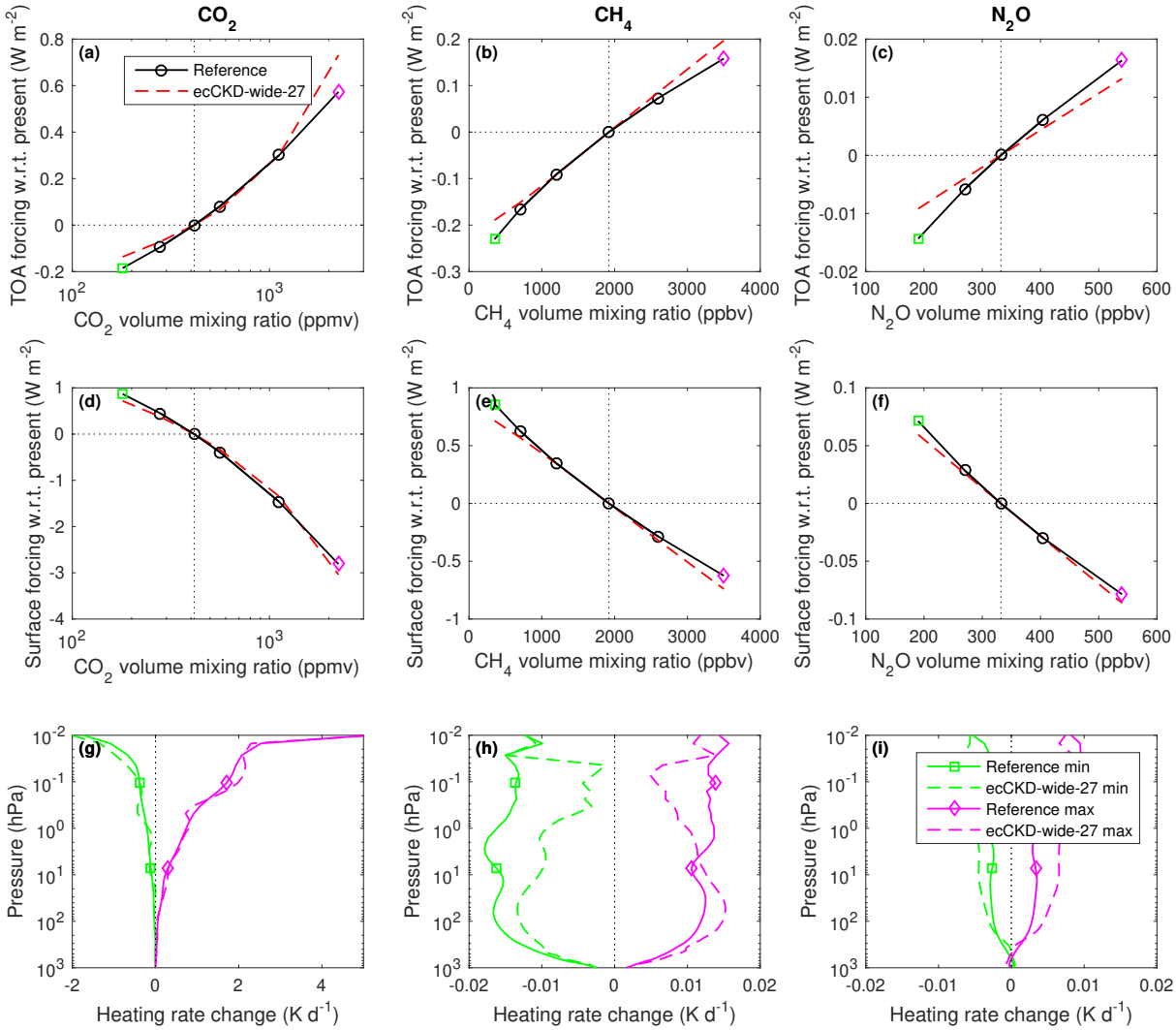

Comparison of reference line-by-line and calculations by the climate-wide-27 model of the instantaneous clear-sky radiative forcing from perturbing each of the five well-mixed greenhouse gases from their present-day values, at (top row) top-of-atmosphere and (middle row) surface, averaged over the 50 profiles of the Evaluation-1 dataset. The bottom row shows the mean change to heating rate resulting from perturbing the concentration of a gas from its present-day value to either the maximum or minimum value in the range for that gas.

Model 4: ecCKD climate-wide-38

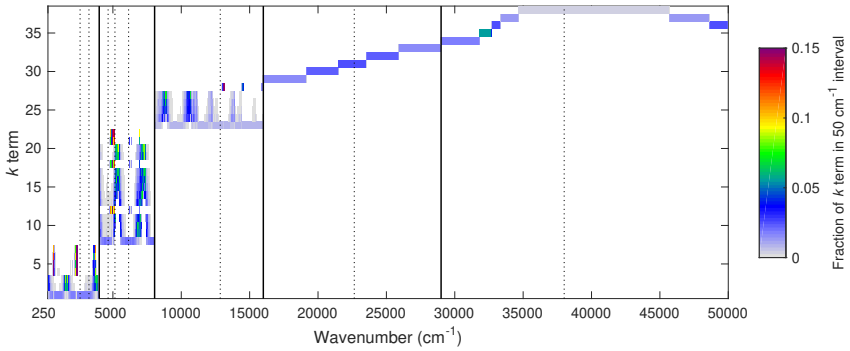

Illustration of the parts of the shortwave spectrum that contribute to each k term of the climate-wide-38 model.

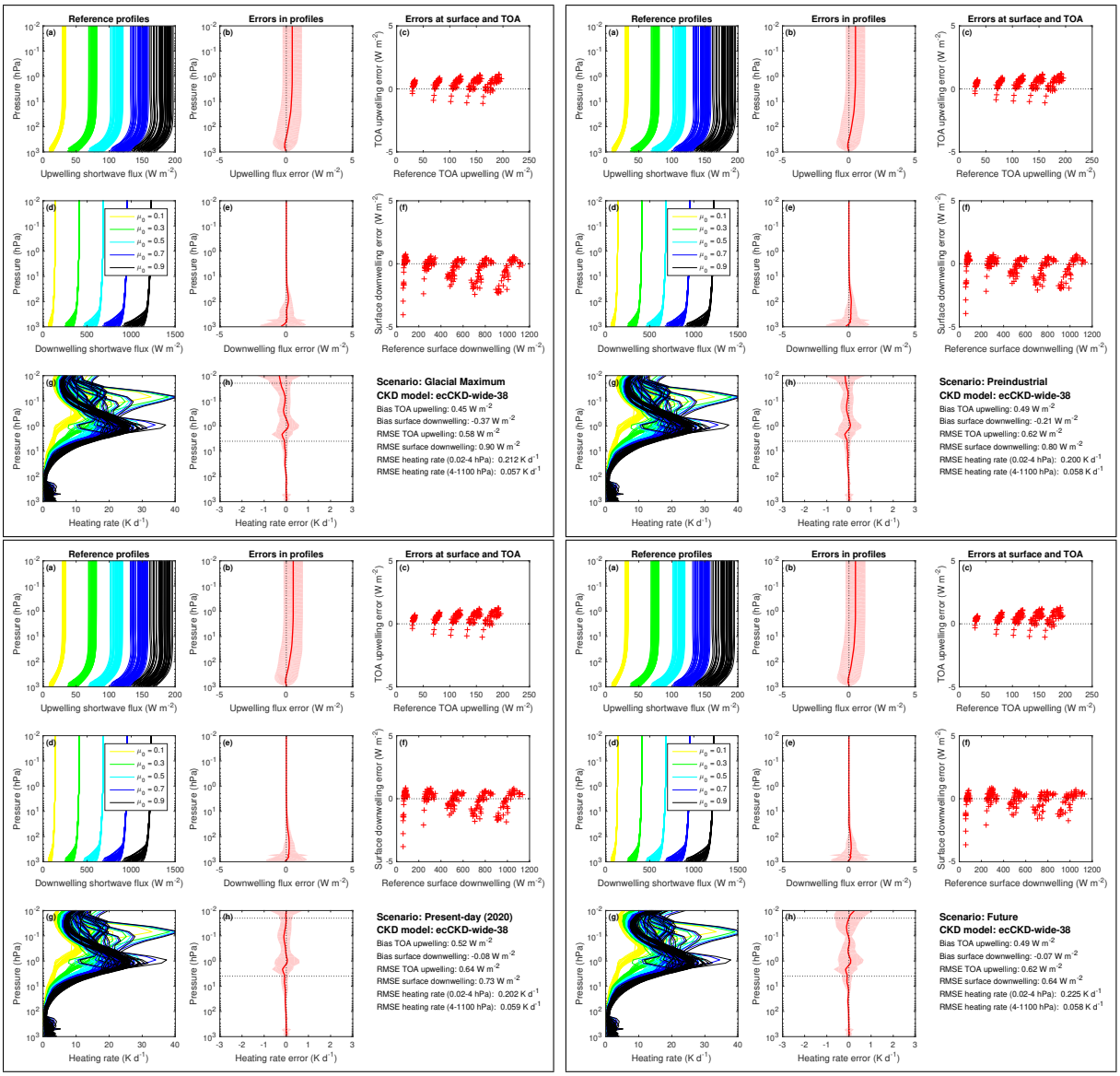

Each boxed group of panels evaluate the climate-wide-38 CKD model for a single CKDMIP scenario. The left three panels in each group show the irradiances and heating rates from the reference line-by-line calculations for five values of the cosine of the solar zenith angle, μ_0. The red lines in the middle three panels show the corresponding bias in these quantities from the CKD model. The shaded regions encompass 95% of the instantaneous errors. Panels c and f depict instantaneous errors in upwelling TOA and downwelling surface irradiances.

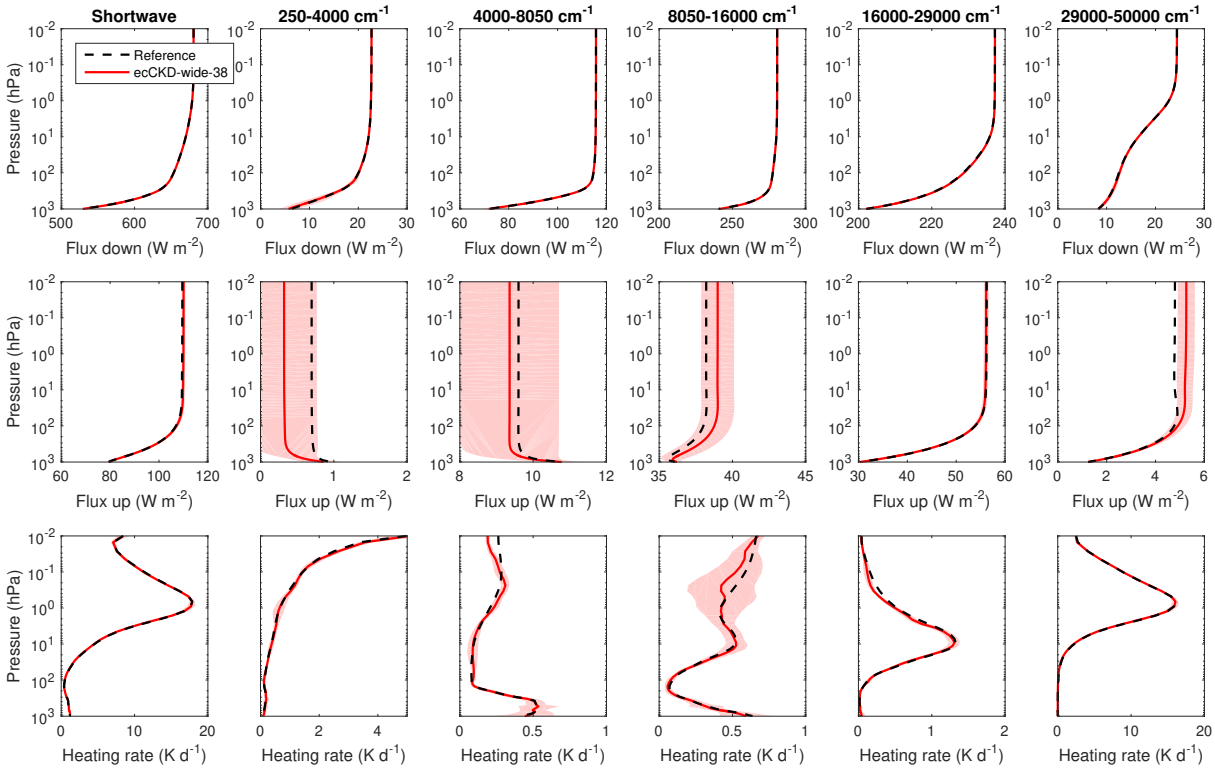

Evaluation of irradiances and heating rates for the broadband (leftmost column of panels) and the 5 wide shortwave bands (other panels) of the climate-wide-38 CKD model. The black dashed and red solid lines correspond to the average of the 50 profiles for the "present-day" scenario, while the shaded regions encompass 95% of the error.

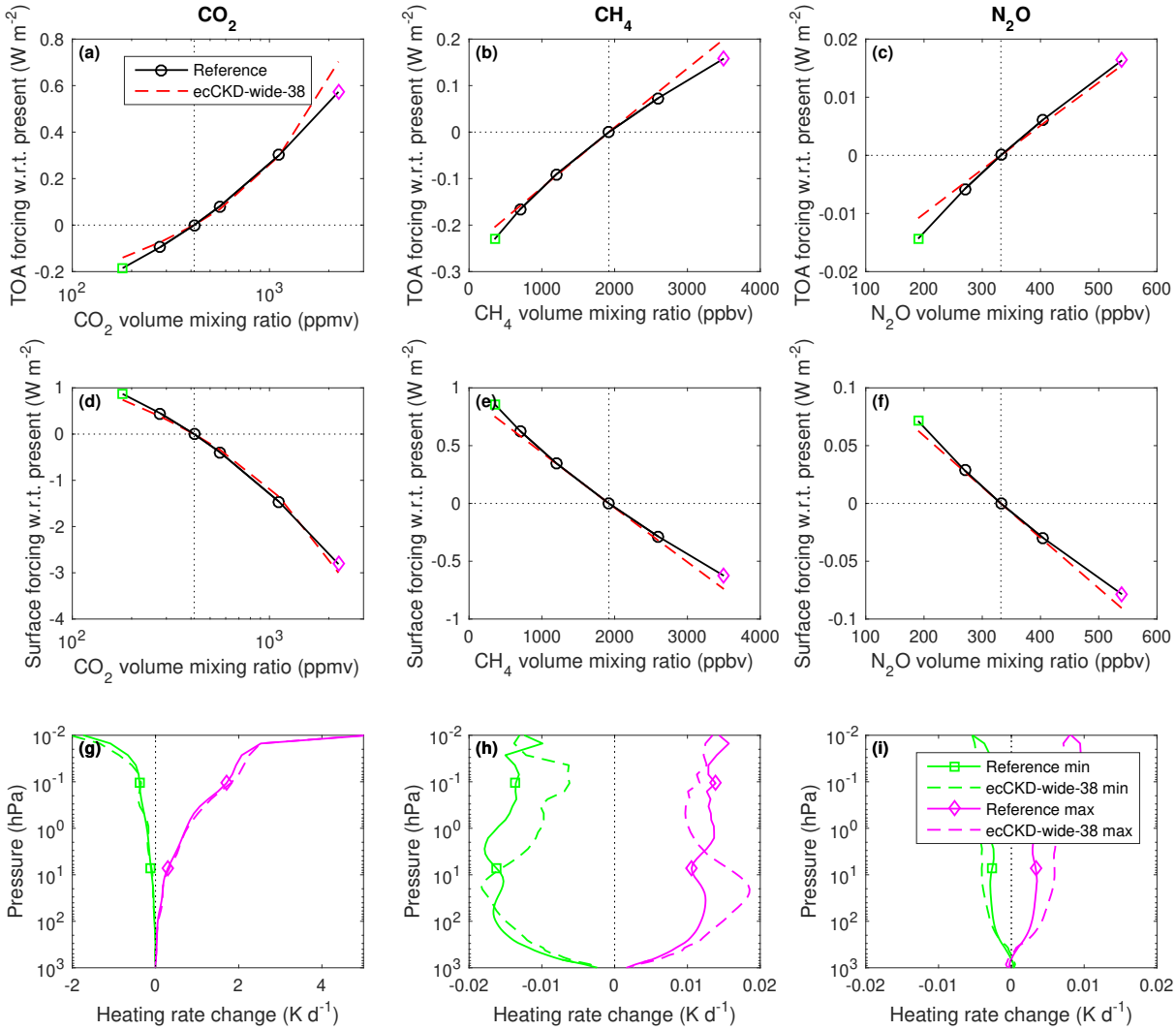

Comparison of reference line-by-line and calculations by the climate-wide-38 model of the instantaneous clear-sky radiative forcing from perturbing each of the five well-mixed greenhouse gases from their present-day values, at (top row) top-of-atmosphere and (middle row) surface, averaged over the 50 profiles of the Evaluation-1 dataset. The bottom row shows the mean change to heating rate resulting from perturbing the concentration of a gas from its present-day value to either the maximum or minimum value in the range for that gas.

Model 5: ecCKD climate-wide-60

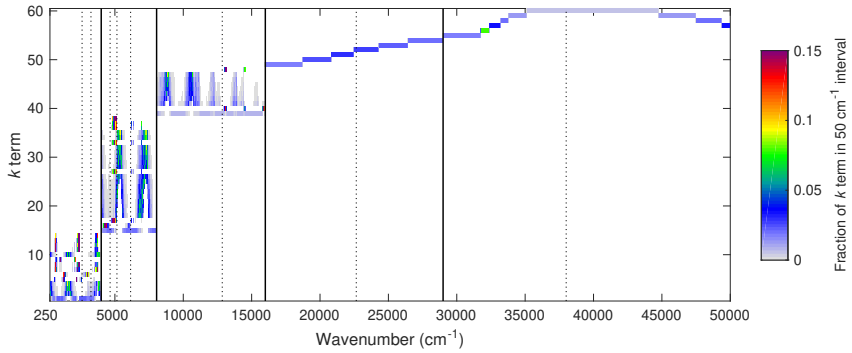

Illustration of the parts of the shortwave spectrum that contribute to each k term of the climate-wide-60 model.

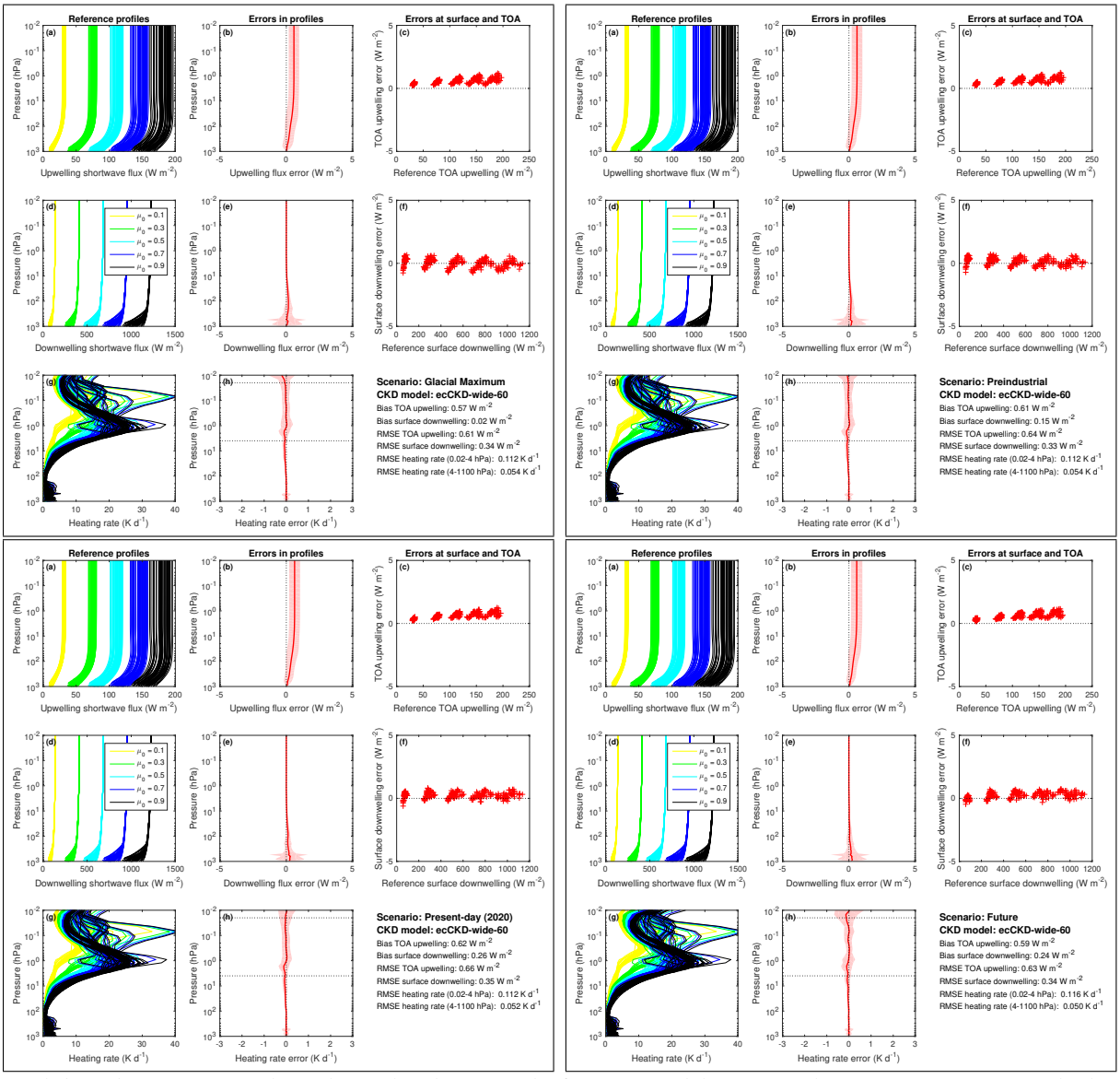

Each boxed group of panels evaluate the climate-wide-60 CKD model for a single CKDMIP scenario. The left three panels in each group show the irradiances and heating rates from the reference line-by-line calculations for five values of the cosine of the solar zenith angle, μ_0. The red lines in the middle three panels show the corresponding bias in these quantities from the CKD model. The shaded regions encompass 95% of the instantaneous errors. Panels c and f depict instantaneous errors in upwelling TOA and downwelling surface irradiances.

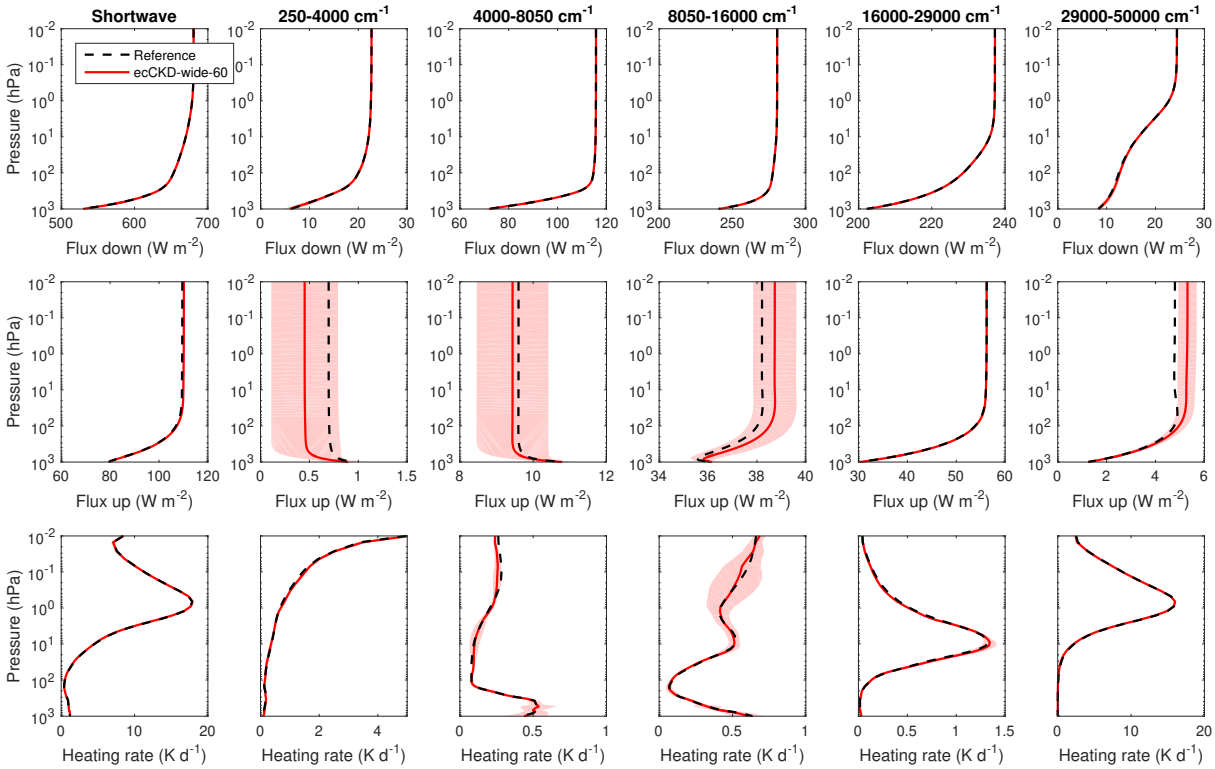

Evaluation of irradiances and heating rates for the broadband (leftmost column of panels) and the 5 wide shortwave bands (other panels) of the climate-wide-60 CKD model. The black dashed and red solid lines correspond to the average of the 50 profiles for the "present-day" scenario, while the shaded regions encompass 95% of the error.

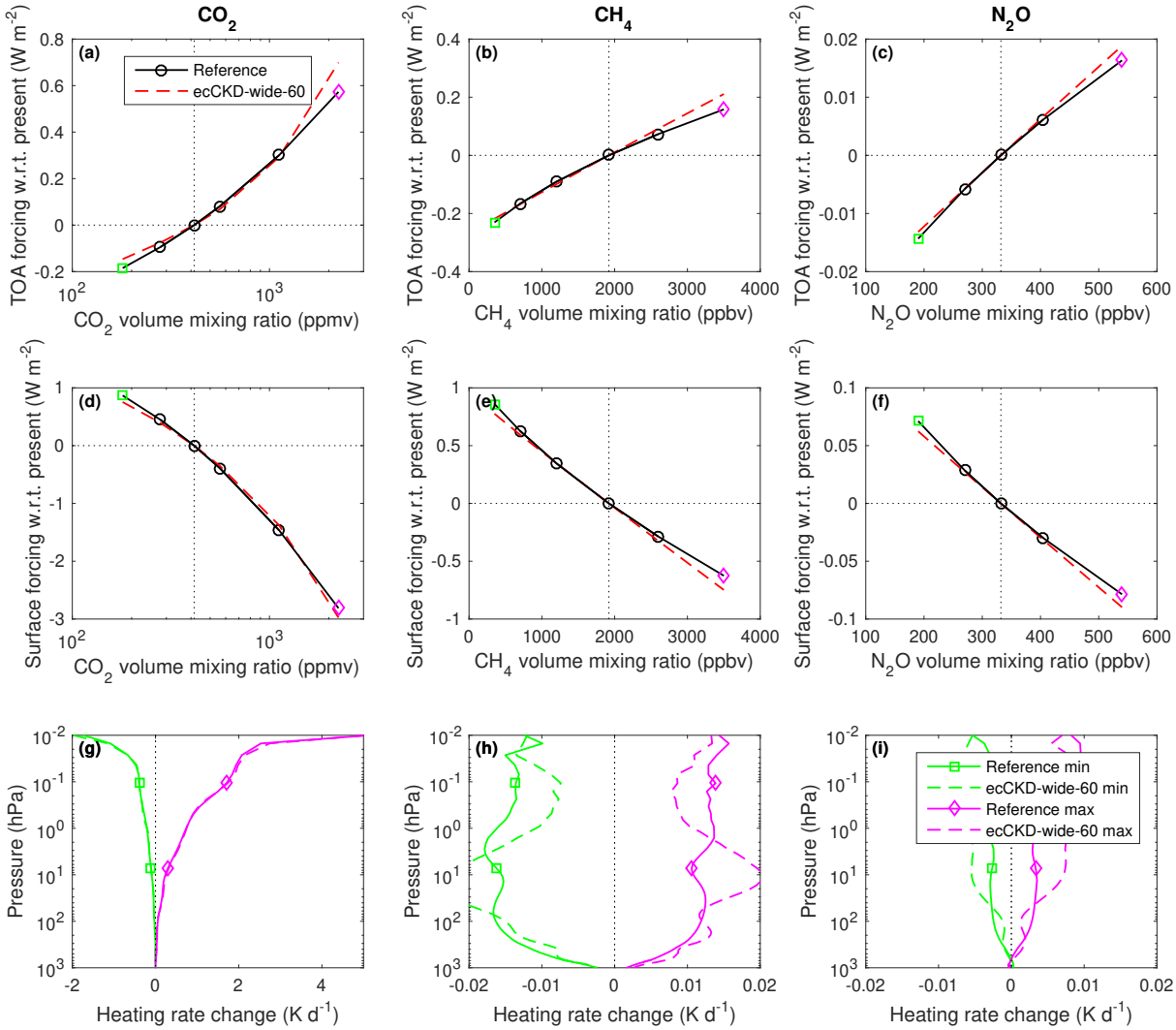

Comparison of reference line-by-line and calculations by the climate-wide-60 model of the instantaneous clear-sky radiative forcing from perturbing each of the five well-mixed greenhouse gases from their present-day values, at (top row) top-of-atmosphere and (middle row) surface, averaged over the 50 profiles of the Evaluation-1 dataset. The bottom row shows the mean change to heating rate resulting from perturbing the concentration of a gas from its present-day value to either the maximum or minimum value in the range for that gas.

Model 6: ecCKD climate-wide-84

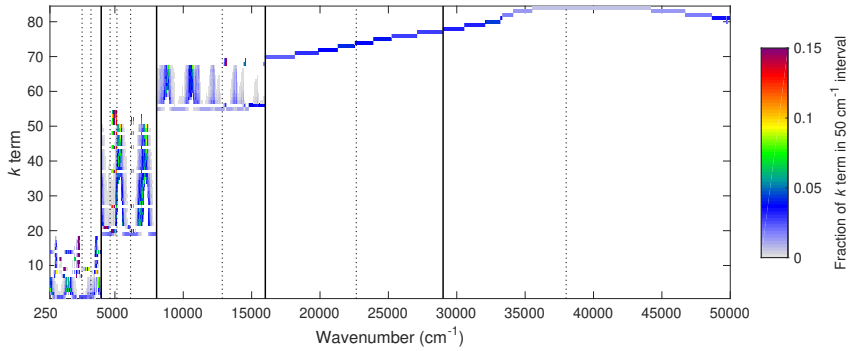

Illustration of the parts of the shortwave spectrum that contribute to each k term of the climate-wide-84 model.

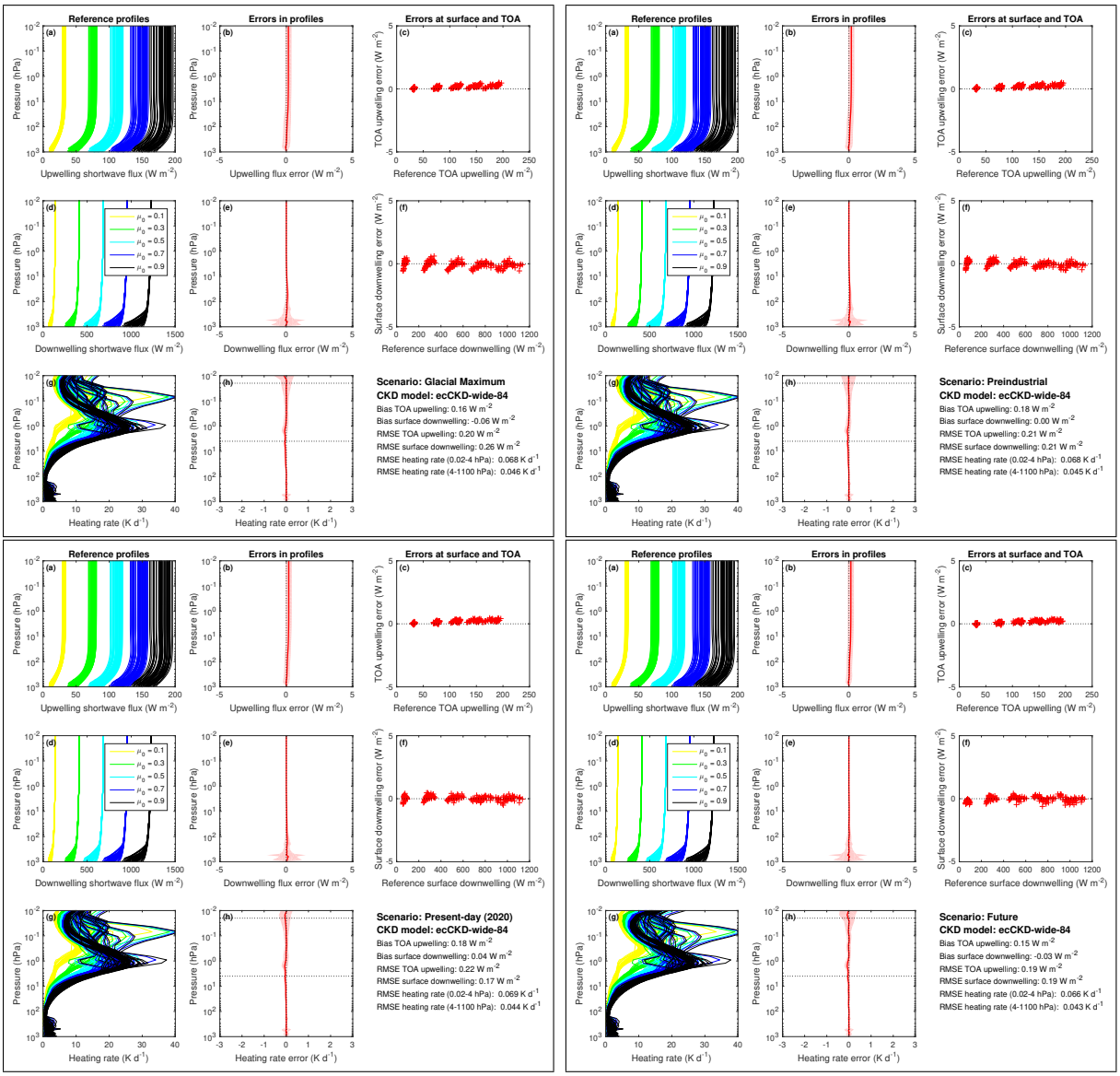

Each boxed group of panels evaluate the climate-wide-84 CKD model for a single CKDMIP scenario. The left three panels in each group show the irradiances and heating rates from the reference line-by-line calculations for five values of the cosine of the solar zenith angle, μ_0. The red lines in the middle three panels show the corresponding bias in these quantities from the CKD model. The shaded regions encompass 95% of the instantaneous errors. Panels c and f depict instantaneous errors in upwelling TOA and downwelling surface irradiances.

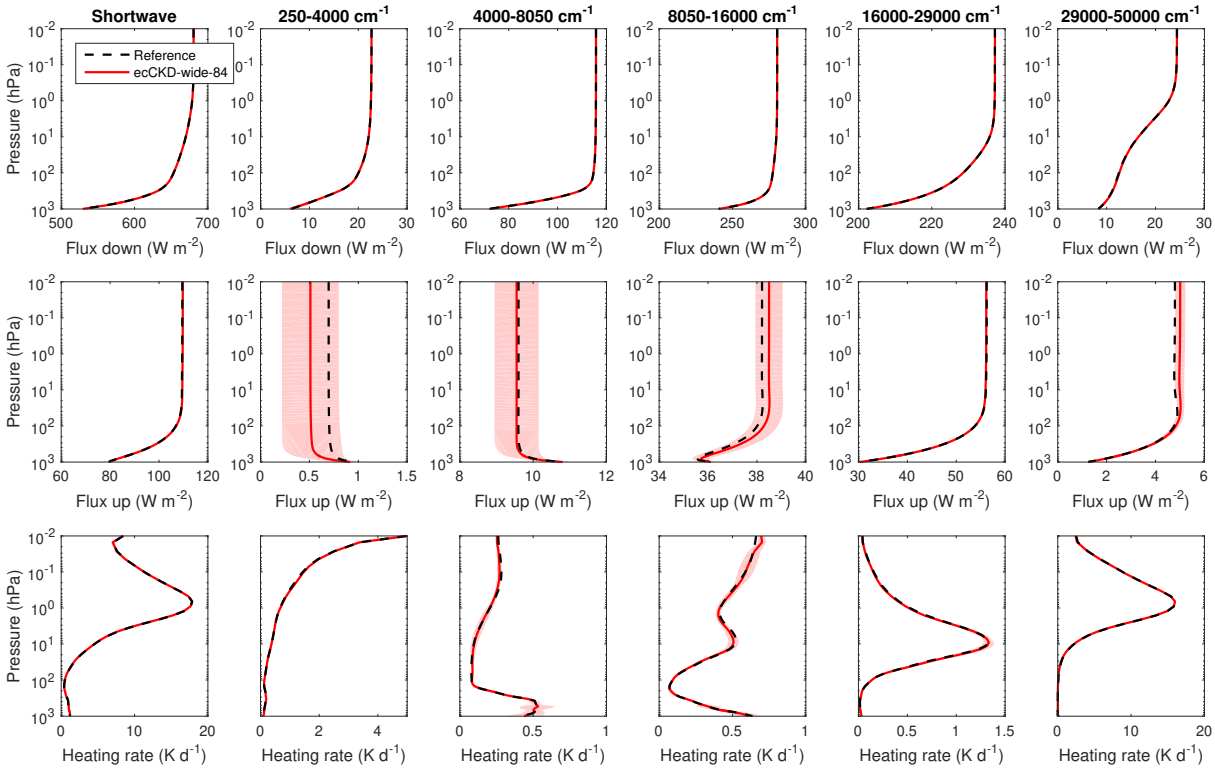

Evaluation of irradiances and heating rates for the broadband (leftmost column of panels) and the 5 wide shortwave bands (other panels) of the climate-wide-84 CKD model. The black dashed and red solid lines correspond to the average of the 50 profiles for the "present-day" scenario, while the shaded regions encompass 95% of the error.

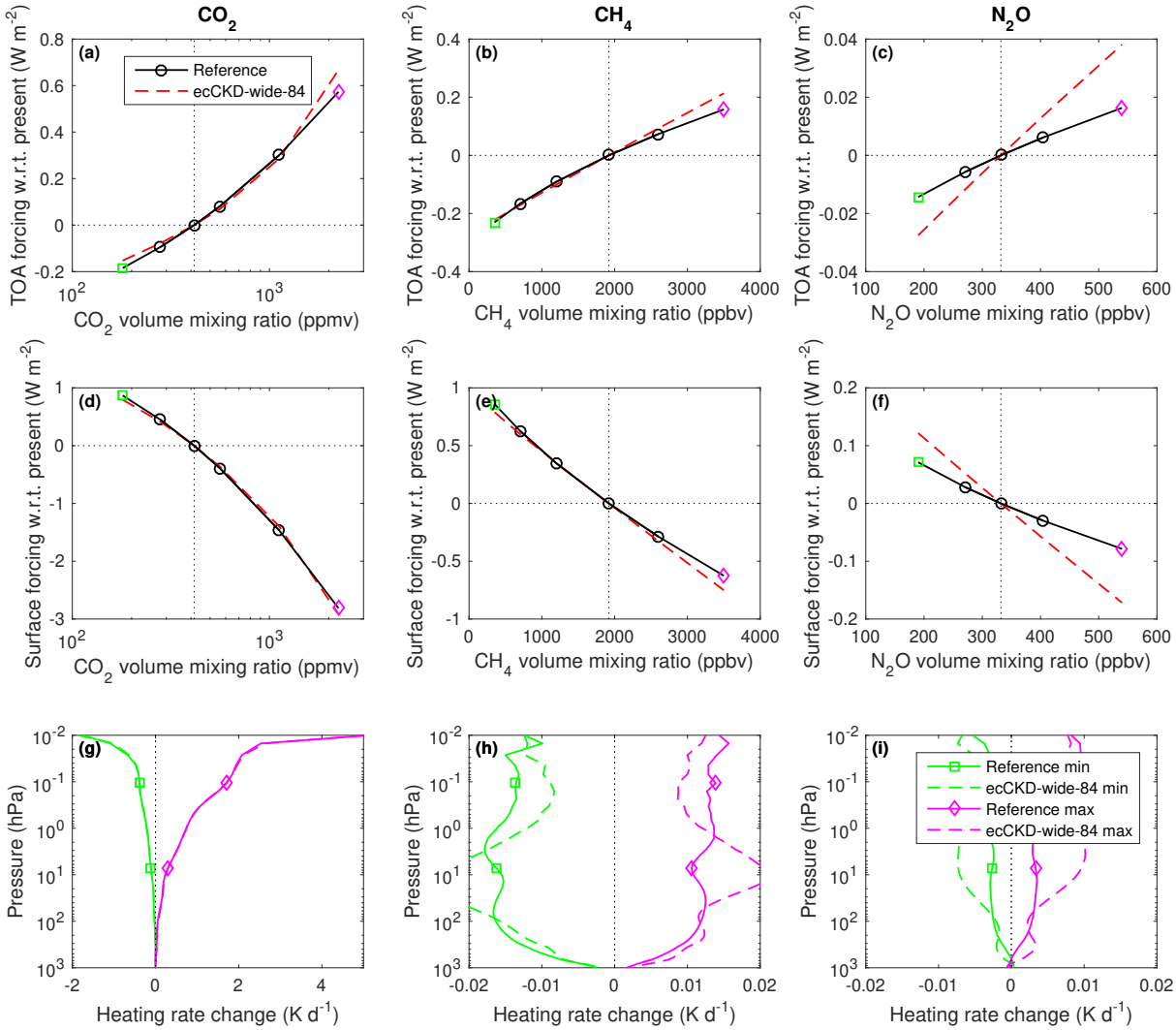

Comparison of reference line-by-line and calculations by the climate-wide-84 model of the instantaneous clear-sky radiative forcing from perturbing each of the five well-mixed greenhouse gases from their present-day values, at (top row) top-of-atmosphere and (middle row) surface, averaged over the 50 profiles of the Evaluation-1 dataset. The bottom row shows the mean change to heating rate resulting from perturbing the concentration of a gas from its present-day value to either the maximum or minimum value in the range for that gas.

Model 7: ecCKD climate-narrow-16

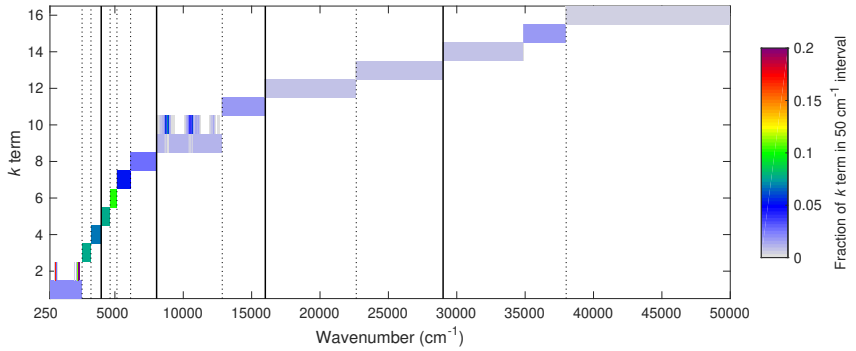

Illustration of the parts of the shortwave spectrum that contribute to each k term of the climate-narrow-16 model.

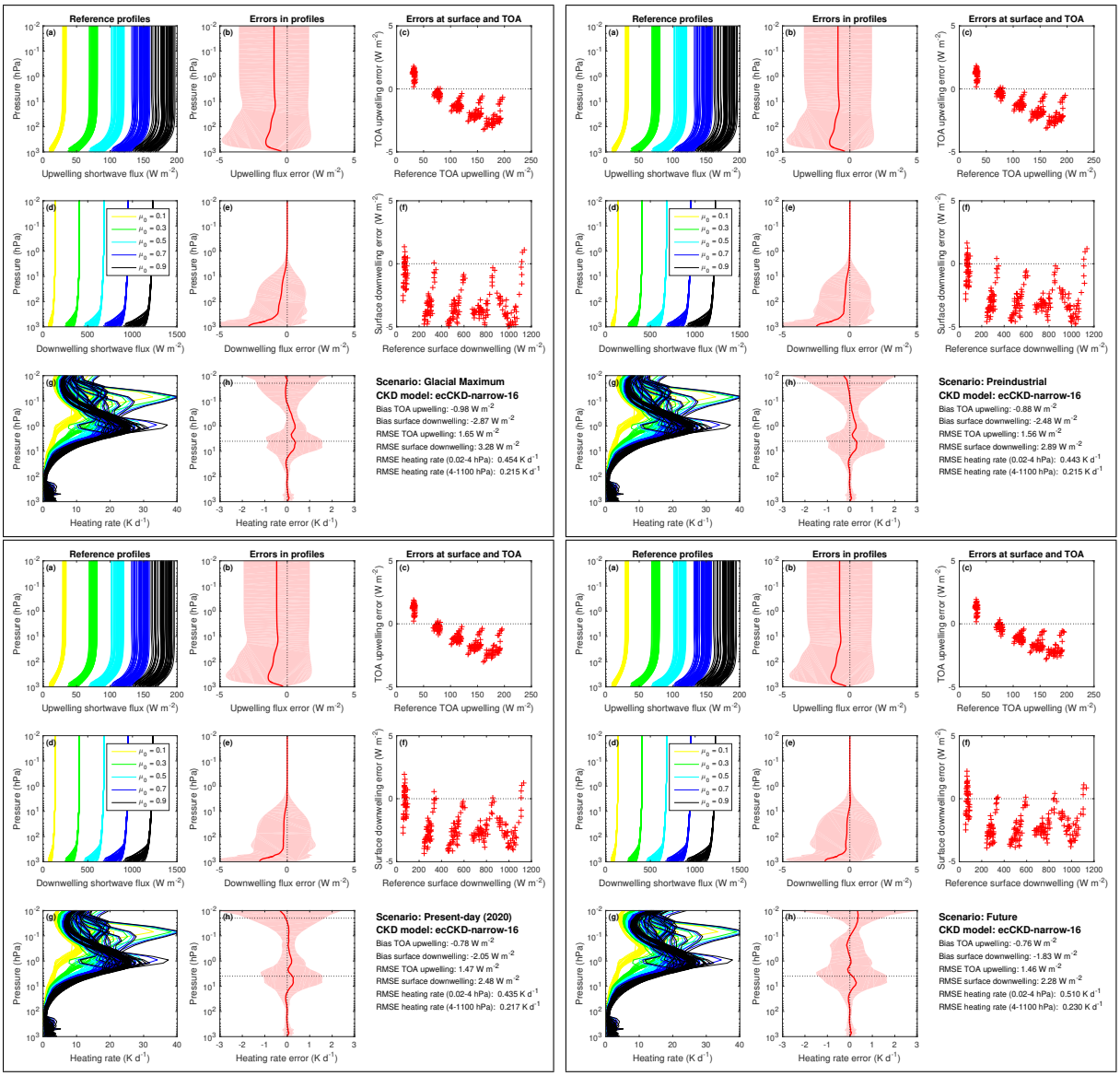

Each boxed group of panels evaluate the climate-narrow-16 CKD model for a single CKDMIP scenario. The left three panels in each group show the irradiances and heating rates from the reference line-by-line calculations for five values of the cosine of the solar zenith angle, μ_0. The red lines in the middle three panels show the corresponding bias in these quantities from the CKD model. The shaded regions encompass 95% of the instantaneous errors. Panels c and f depict instantaneous errors in upwelling TOA and downwelling surface irradiances.

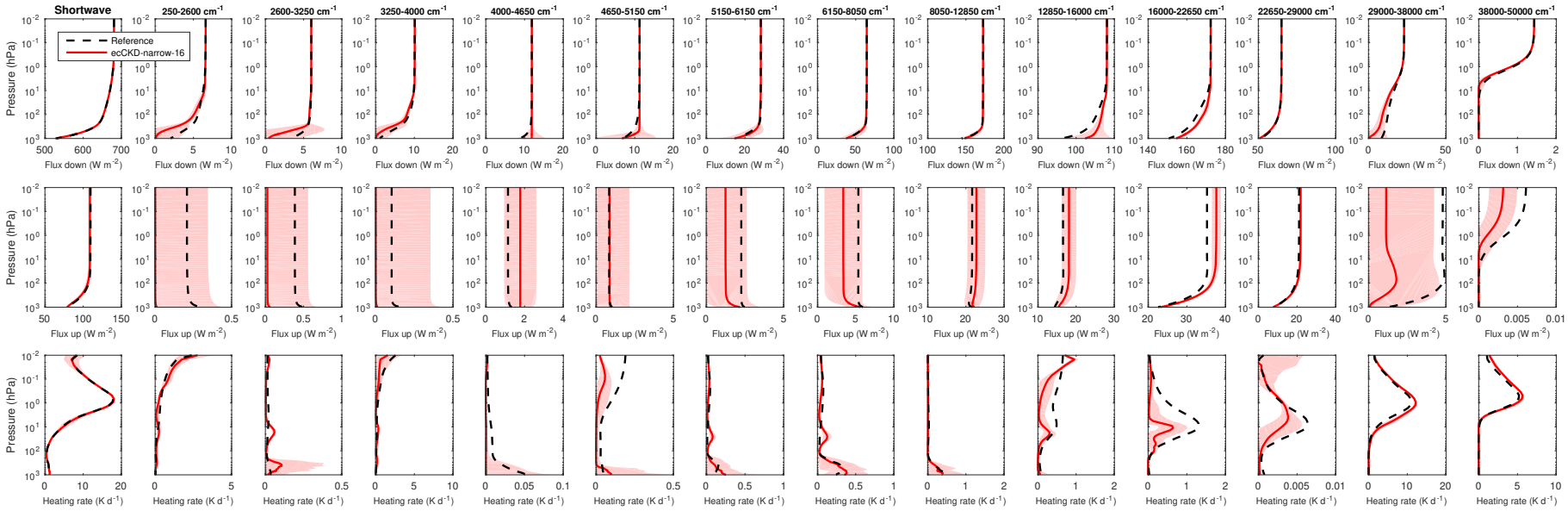

Evaluation of irradiances and heating rates for the broadband (leftmost column of panels) and the 13 narrow shortwave bands (other panels) of the climate-narrow-16 CKD model. The black dashed and red solid lines correspond to the average of the 50 profiles for the "present-day" scenario, while the shaded regions encompass 95% of the error.

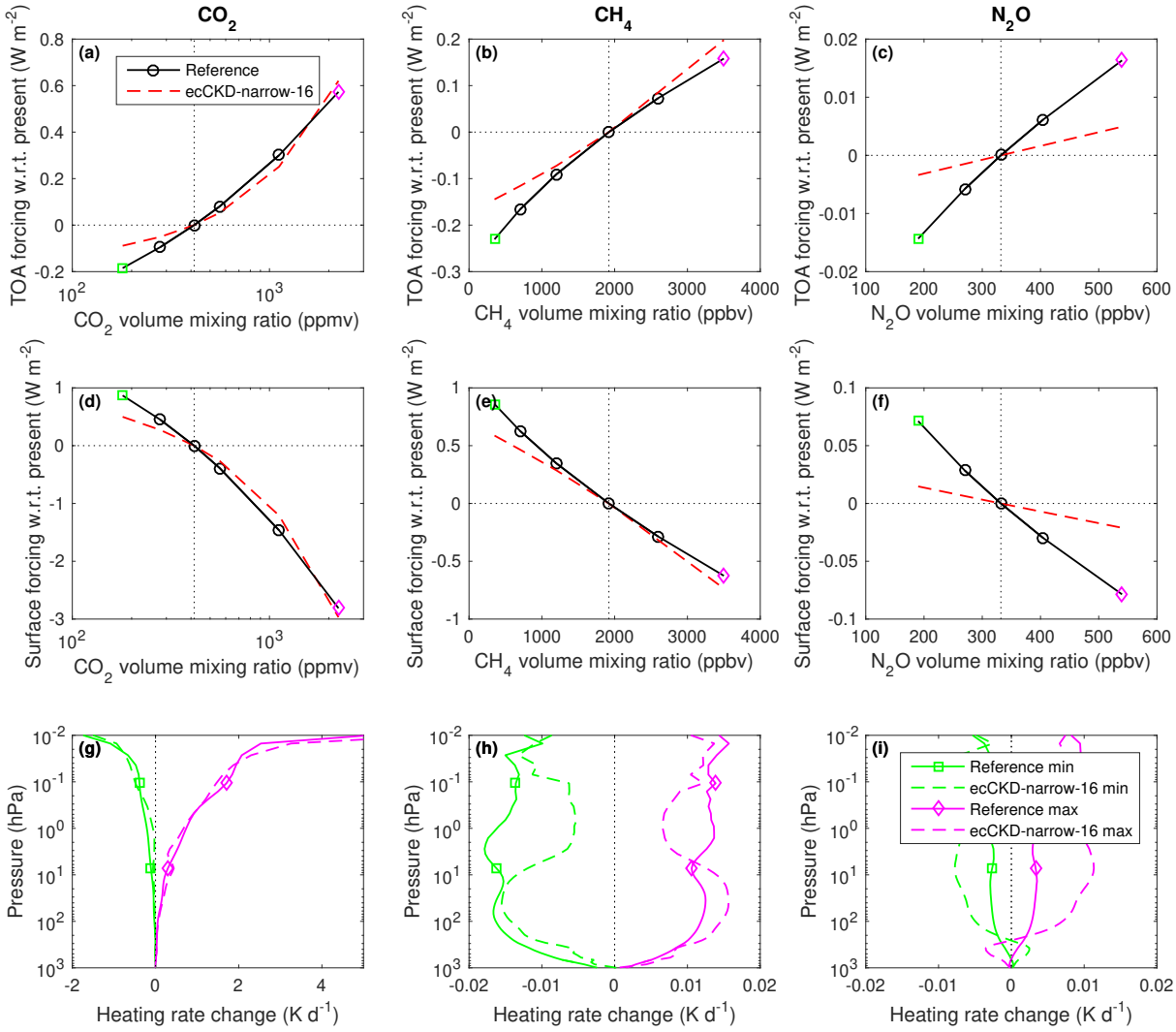

Comparison of reference line-by-line and calculations by the climate-narrow-16 model of the instantaneous clear-sky radiative forcing from perturbing each of the five well-mixed greenhouse gases from their present-day values, at (top row) top-of-atmosphere and (middle row) surface, averaged over the 50 profiles of the Evaluation-1 dataset. The bottom row shows the mean change to heating rate resulting from perturbing the concentration of a gas from its present-day value to either the maximum or minimum value in the range for that gas.

Model 8: ecCKD climate-narrow-23

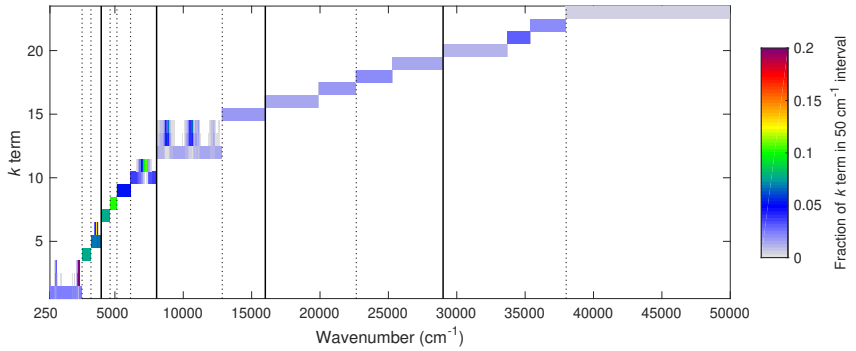

Illustration of the parts of the shortwave spectrum that contribute to each k term of the climate-narrow-23 model.

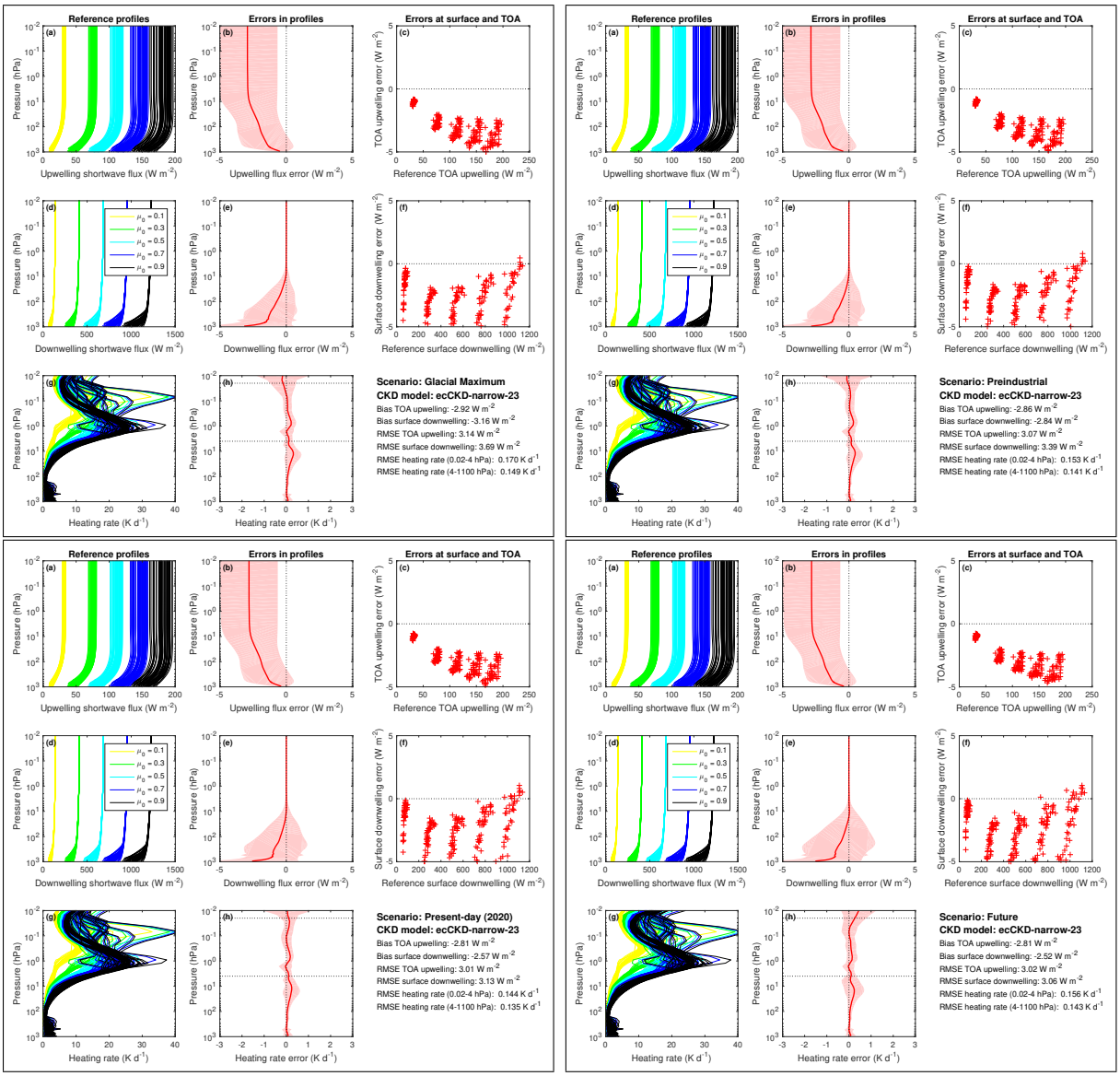

Each boxed group of panels evaluate the climate-narrow-23 CKD model for a single CKDMIP scenario. The left three panels in each group show the irradiances and heating rates from the reference line-by-line calculations for five values of the cosine of the solar zenith angle, μ_0. The red lines in the middle three panels show the corresponding bias in these quantities from the CKD model. The shaded regions encompass 95% of the instantaneous errors. Panels c and f depict instantaneous errors in upwelling TOA and downwelling surface irradiances.

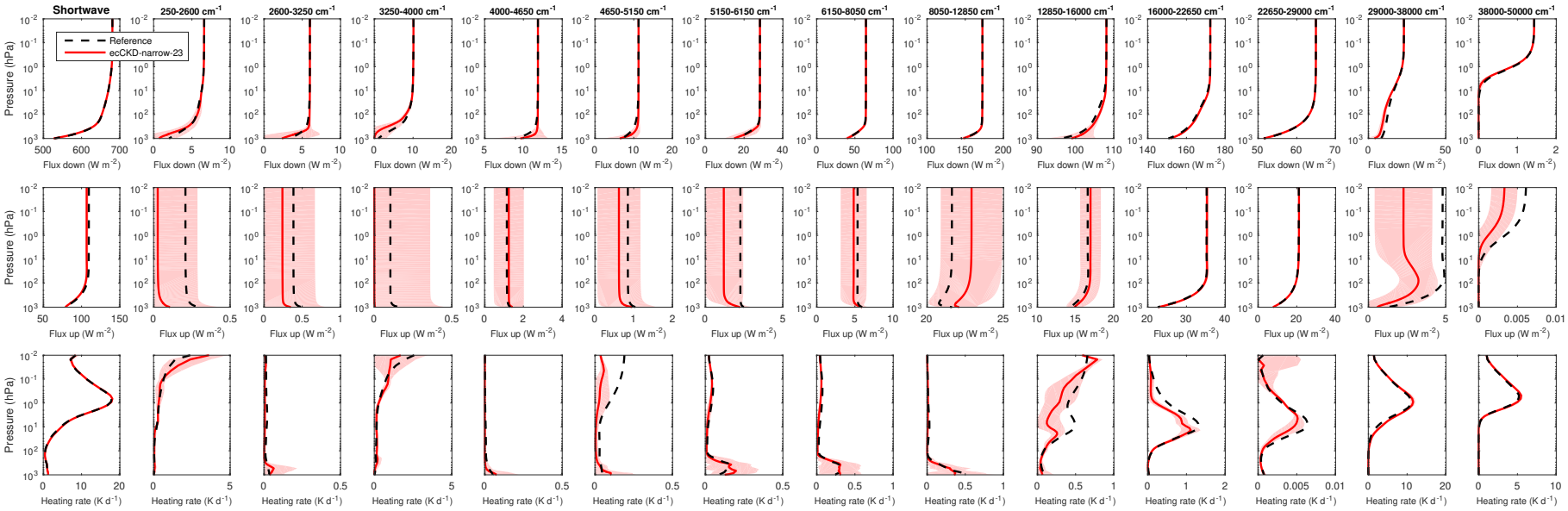

Evaluation of irradiances and heating rates for the broadband (leftmost column of panels) and the 13 narrow shortwave bands (other panels) of the climate-narrow-23 CKD model. The black dashed and red solid lines correspond to the average of the 50 profiles for the "present-day" scenario, while the shaded regions encompass 95% of the error.

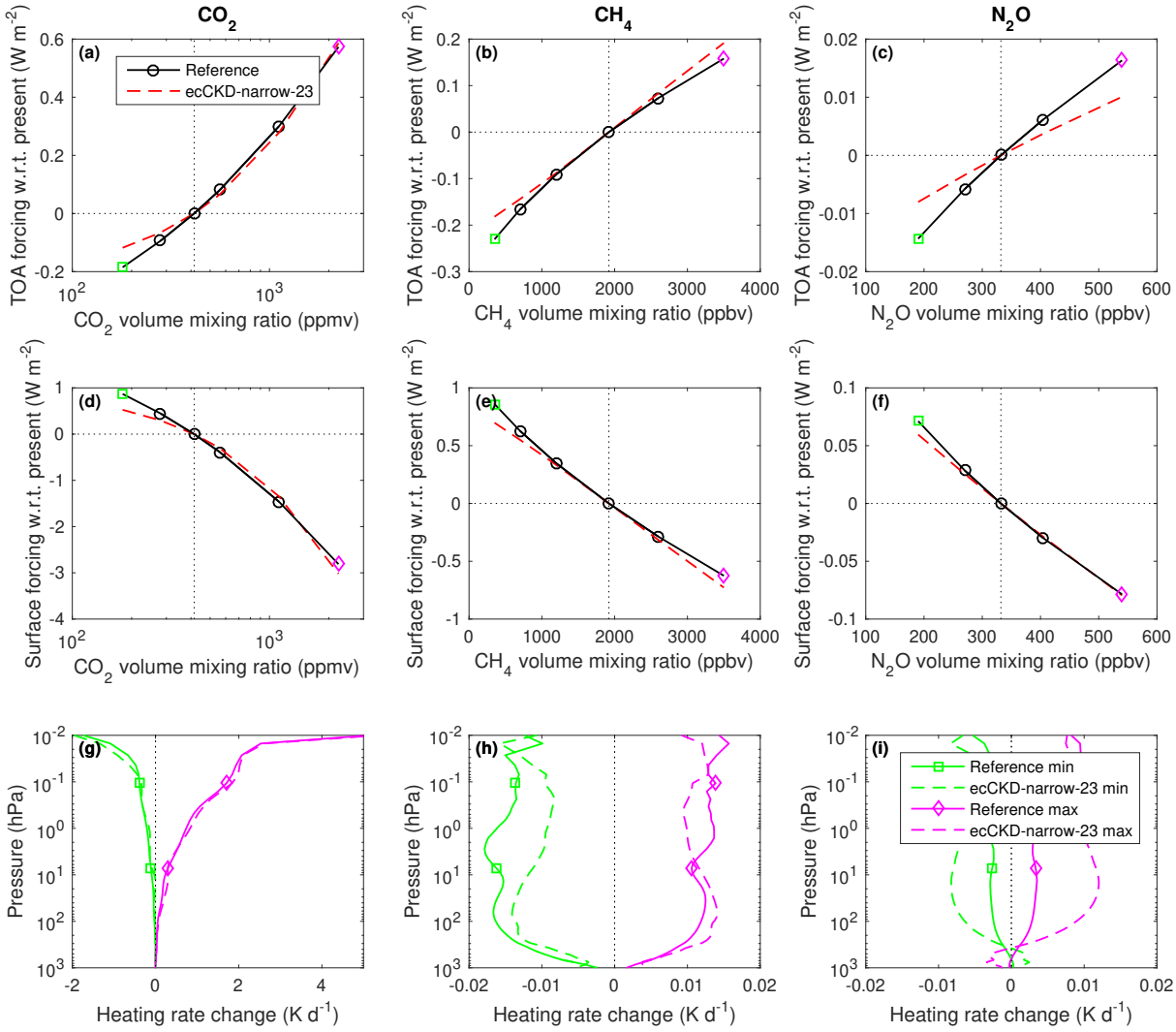

Comparison of reference line-by-line and calculations by the climate-narrow-23 model of the instantaneous clear-sky radiative forcing from perturbing each of the five well-mixed greenhouse gases from their present-day values, at (top row) top-of-atmosphere and (middle row) surface, averaged over the 50 profiles of the Evaluation-1 dataset. The bottom row shows the mean change to heating rate resulting from perturbing the concentration of a gas from its present-day value to either the maximum or minimum value in the range for that gas.

Model 9: ecCKD climate-narrow-25

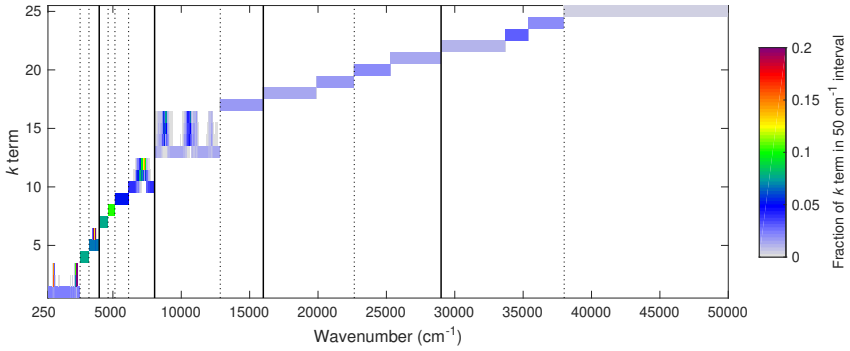

Illustration of the parts of the shortwave spectrum that contribute to each k term of the climate-narrow-25 model.

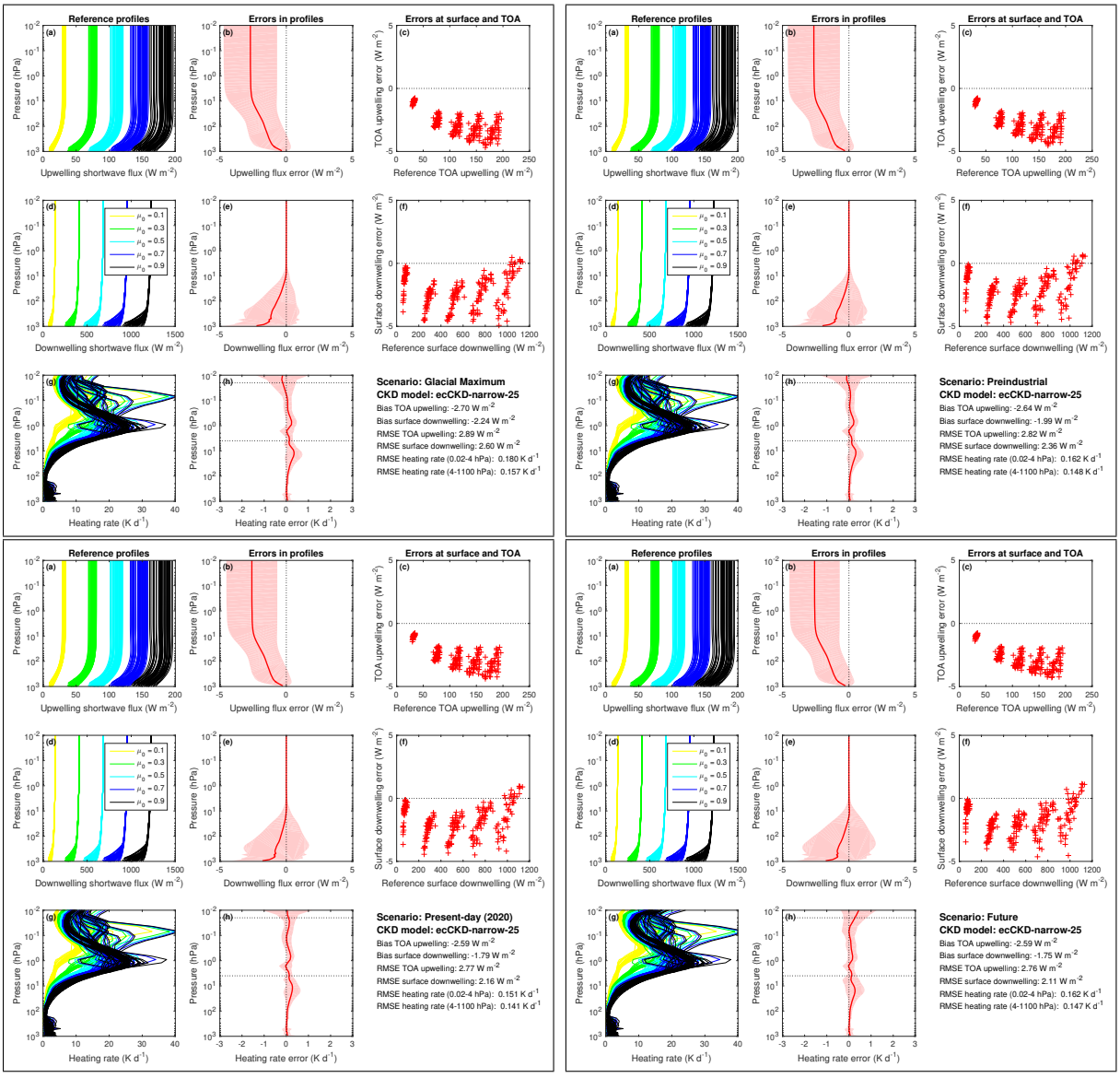

Each boxed group of panels evaluate the climate-narrow-25 CKD model for a single CKDMIP scenario. The left three panels in each group show the irradiances and heating rates from the reference line-by-line calculations for five values of the cosine of the solar zenith angle, μ_0. The red lines in the middle three panels show the corresponding bias in these quantities from the CKD model. The shaded regions encompass 95% of the instantaneous errors. Panels c and f depict instantaneous errors in upwelling TOA and downwelling surface irradiances.

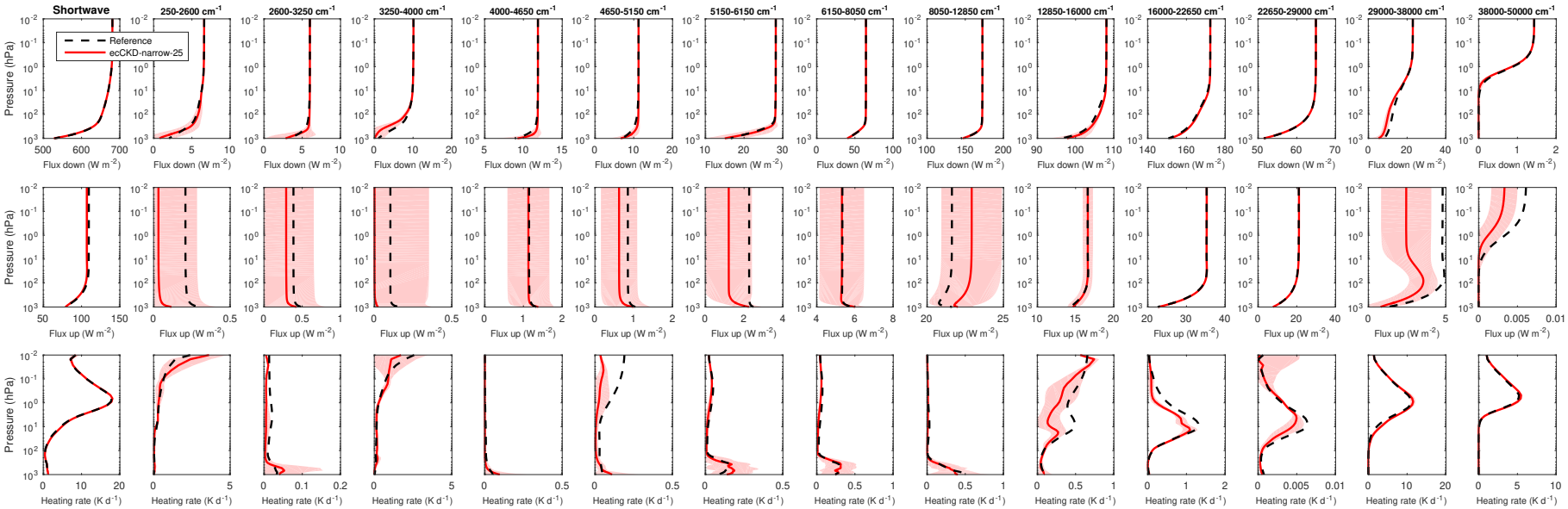

Evaluation of irradiances and heating rates for the broadband (leftmost column of panels) and the 13 narrow shortwave bands (other panels) of the climate-narrow-25 CKD model. The black dashed and red solid lines correspond to the average of the 50 profiles for the "present-day" scenario, while the shaded regions encompass 95% of the error.

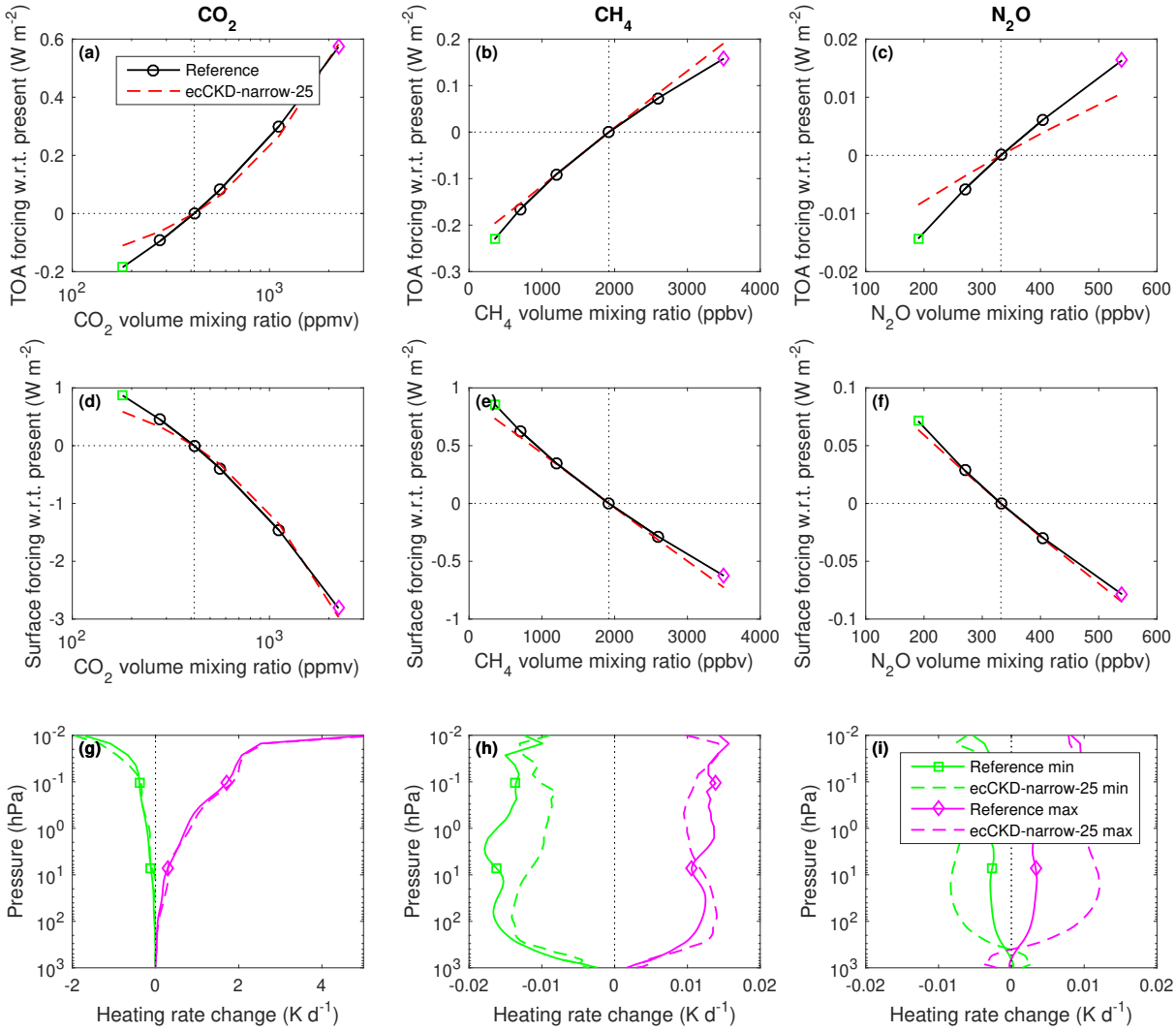

Comparison of reference line-by-line and calculations by the climate-narrow-25 model of the instantaneous clear-sky radiative forcing from perturbing each of the five well-mixed greenhouse gases from their present-day values, at (top row) top-of-atmosphere and (middle row) surface, averaged over the 50 profiles of the Evaluation-1 dataset. The bottom row shows the mean change to heating rate resulting from perturbing the concentration of a gas from its present-day value to either the maximum or minimum value in the range for that gas.

Model 10: ecCKD climate-narrow-35

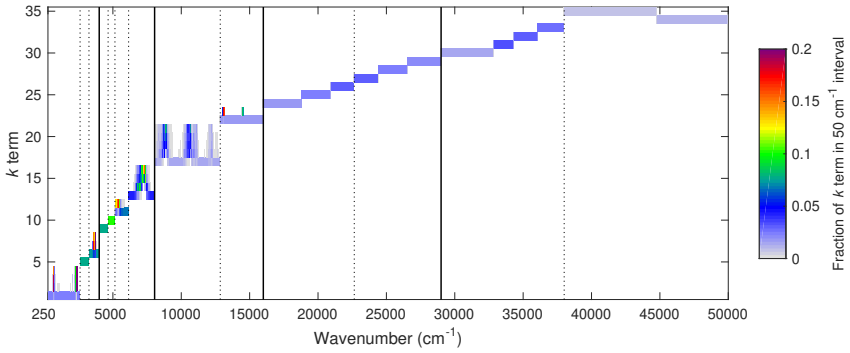

Illustration of the parts of the shortwave spectrum that contribute to each k term of the climate-narrow-35 model.

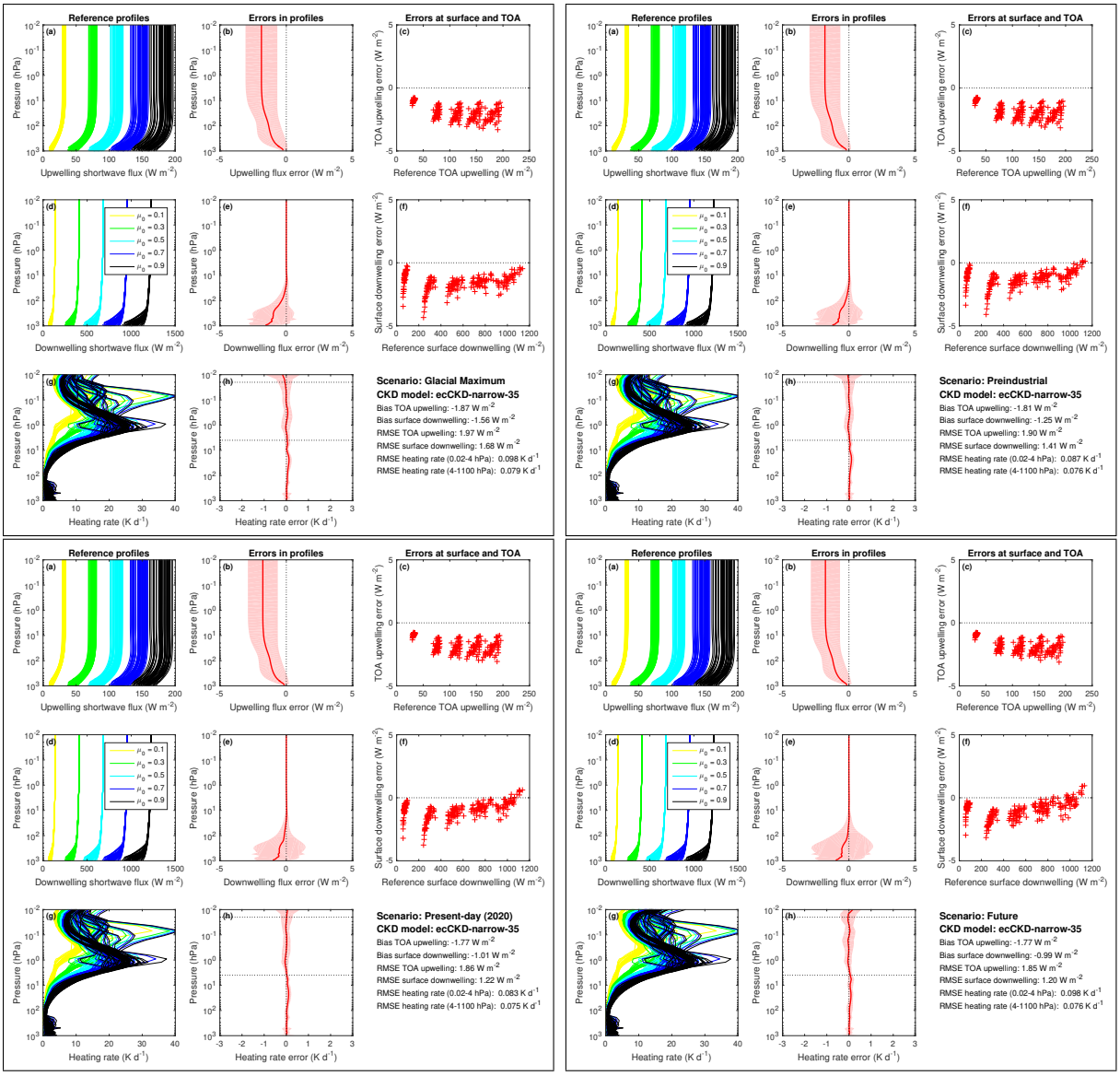

Each boxed group of panels evaluate the climate-narrow-35 CKD model for a single CKDMIP scenario. The left three panels in each group show the irradiances and heating rates from the reference line-by-line calculations for five values of the cosine of the solar zenith angle, μ_0. The red lines in the middle three panels show the corresponding bias in these quantities from the CKD model. The shaded regions encompass 95% of the instantaneous errors. Panels c and f depict instantaneous errors in upwelling TOA and downwelling surface irradiances.

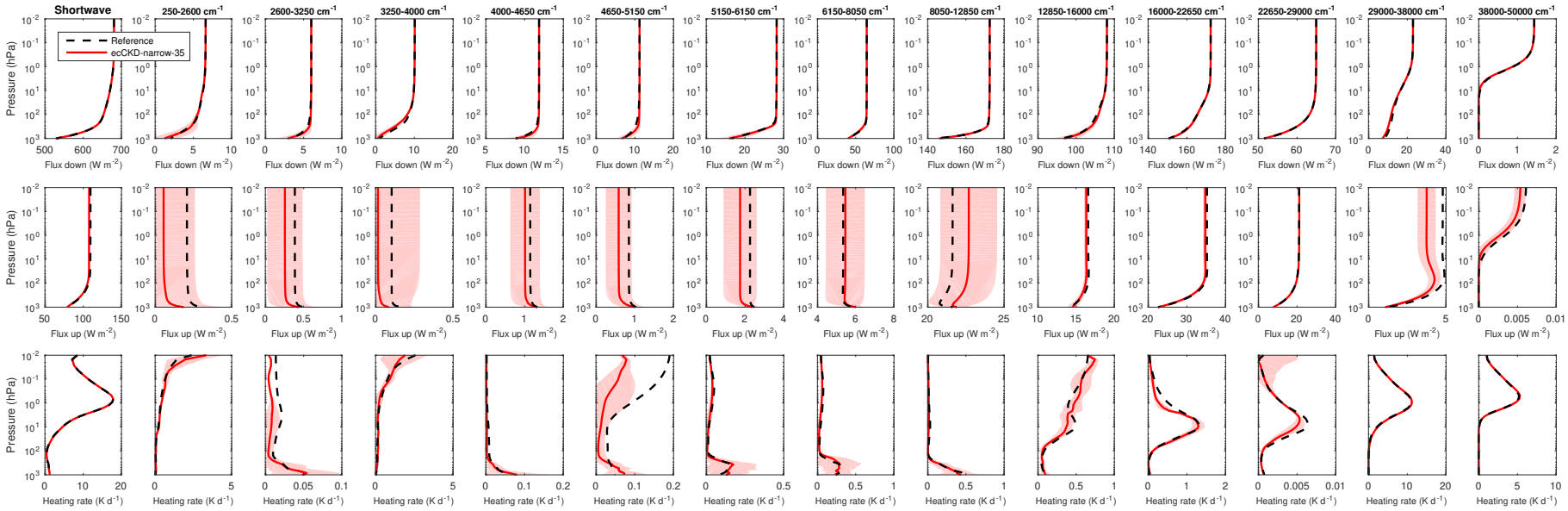

Evaluation of irradiances and heating rates for the broadband (leftmost column of panels) and the 13 narrow shortwave bands (other panels) of the climate-narrow-35 CKD model. The black dashed and red solid lines correspond to the average of the 50 profiles for the "present-day" scenario, while the shaded regions encompass 95% of the error.

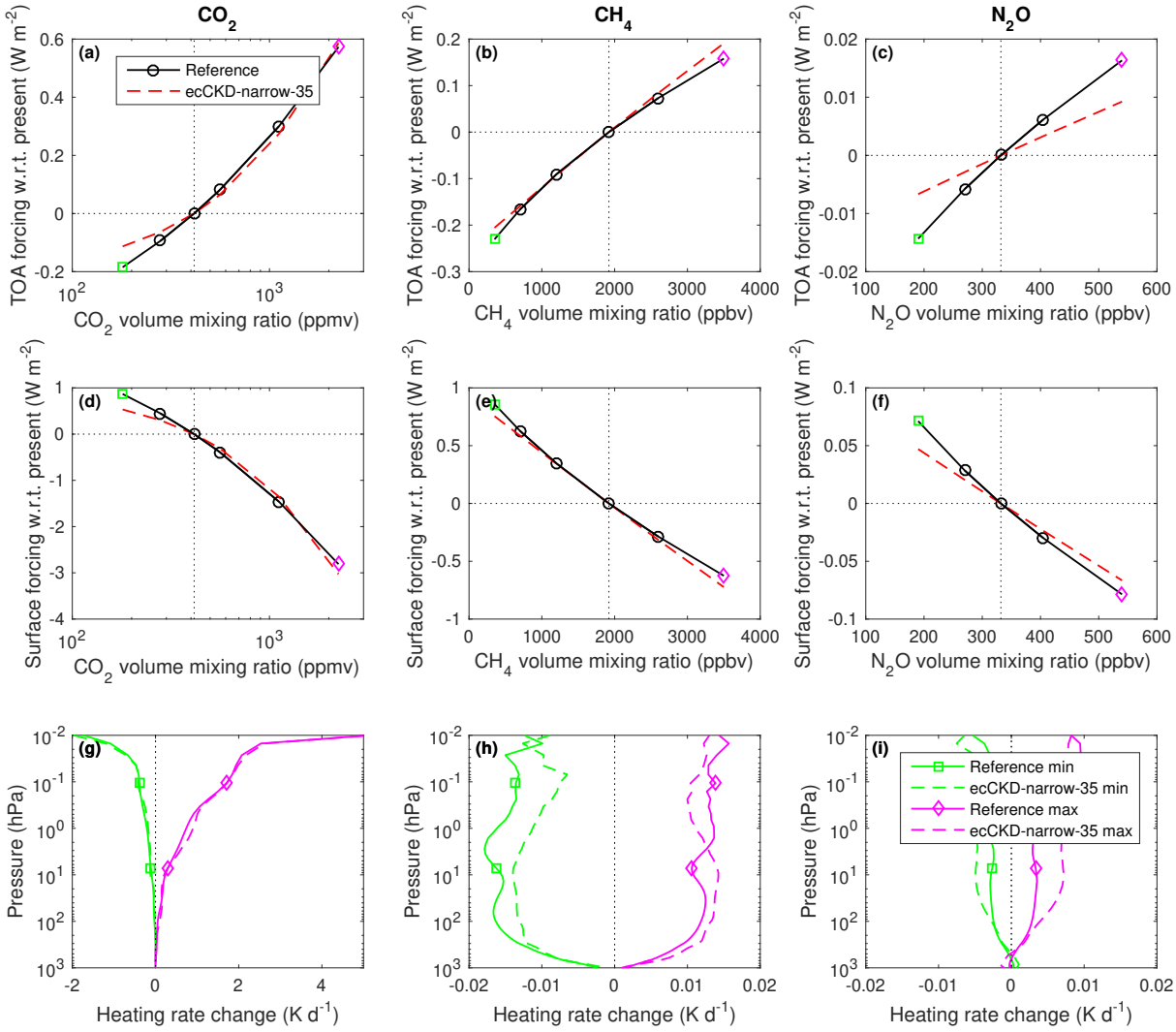

Comparison of reference line-by-line and calculations by the climate-narrow-35 model of the instantaneous clear-sky radiative forcing from perturbing each of the five well-mixed greenhouse gases from their present-day values, at (top row) top-of-atmosphere and (middle row) surface, averaged over the 50 profiles of the Evaluation-1 dataset. The bottom row shows the mean change to heating rate resulting from perturbing the concentration of a gas from its present-day value to either the maximum or minimum value in the range for that gas.

Model 11: ecCKD climate-narrow-47

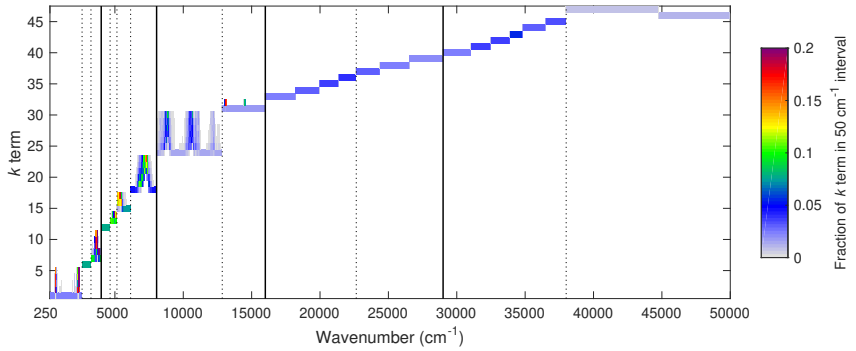

Illustration of the parts of the shortwave spectrum that contribute to each k term of the climate-narrow-47 model.

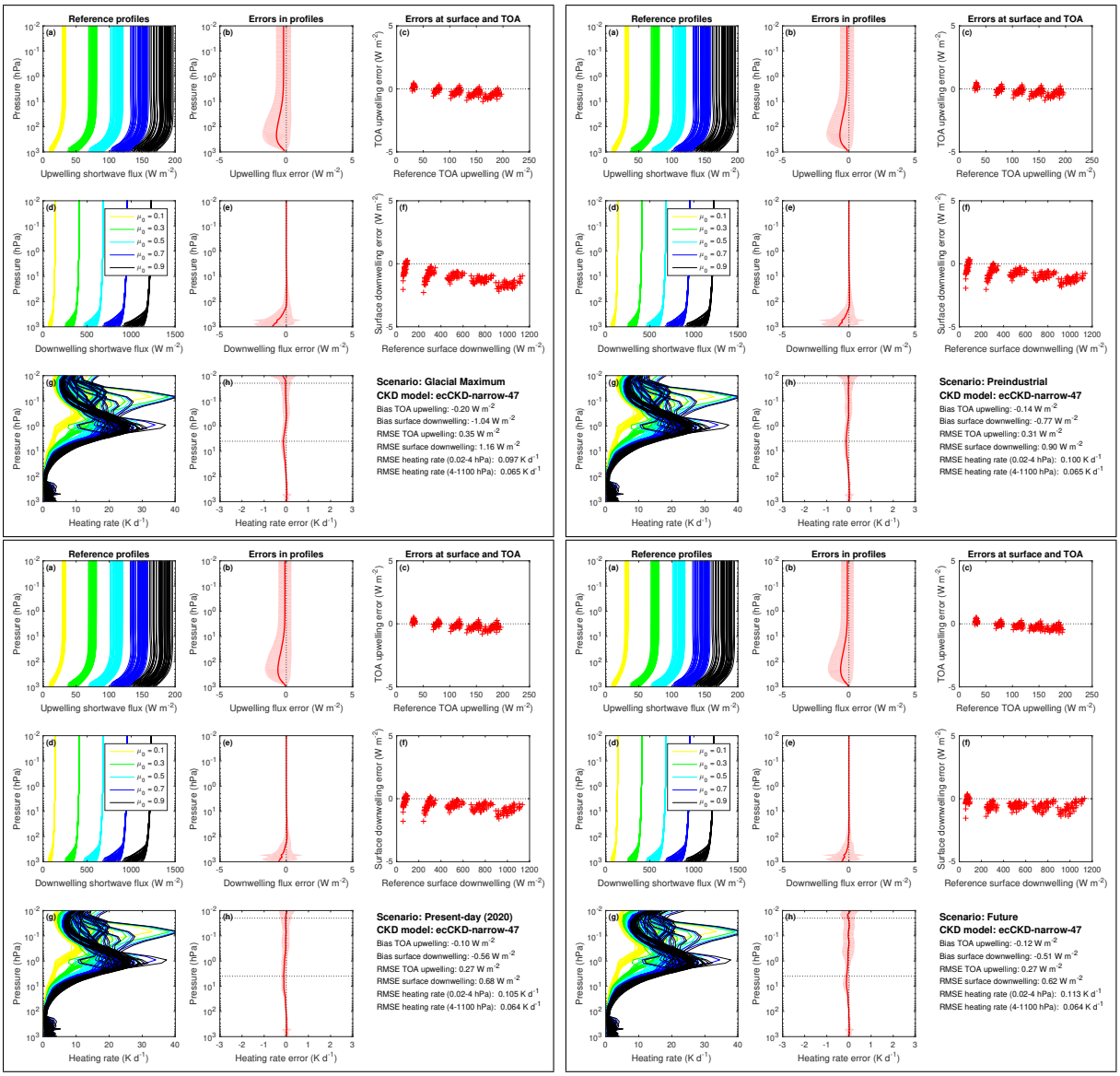

Each boxed group of panels evaluate the climate-narrow-47 CKD model for a single CKDMIP scenario. The left three panels in each group show the irradiances and heating rates from the reference line-by-line calculations for five values of the cosine of the solar zenith angle, μ_0. The red lines in the middle three panels show the corresponding bias in these quantities from the CKD model. The shaded regions encompass 95% of the instantaneous errors. Panels c and f depict instantaneous errors in upwelling TOA and downwelling surface irradiances.

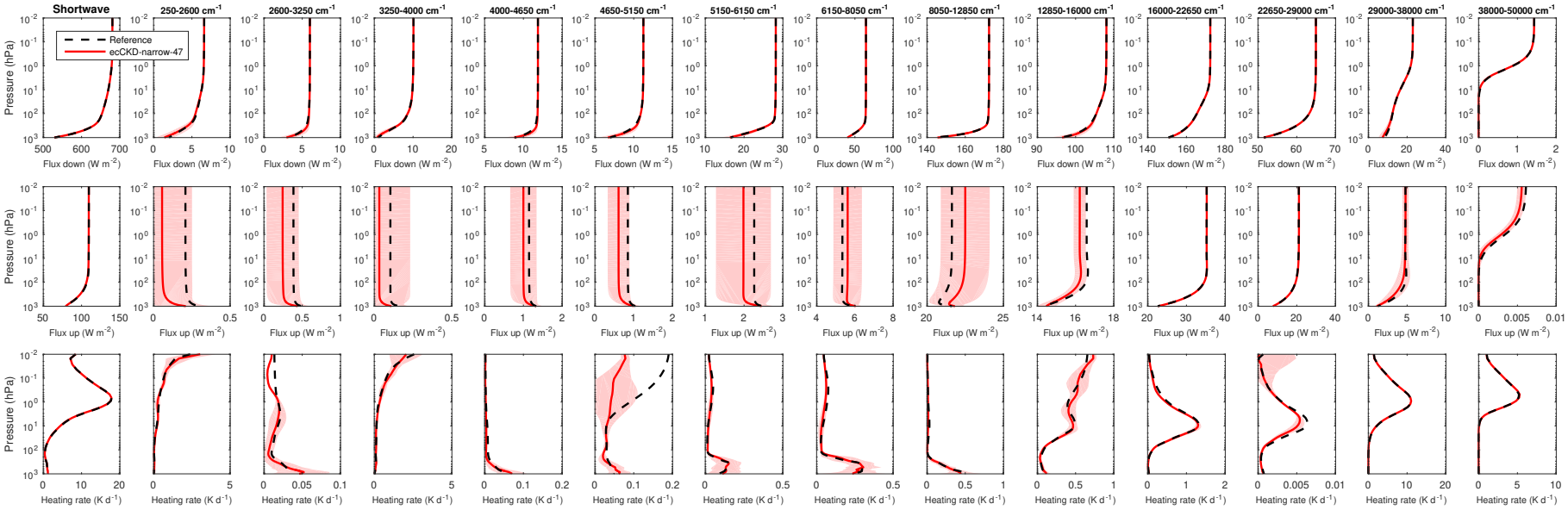

Evaluation of irradiances and heating rates for the broadband (leftmost column of panels) and the 13 narrow shortwave bands (other panels) of the climate-narrow-47 CKD model. The black dashed and red solid lines correspond to the average of the 50 profiles for the "present-day" scenario, while the shaded regions encompass 95% of the error.

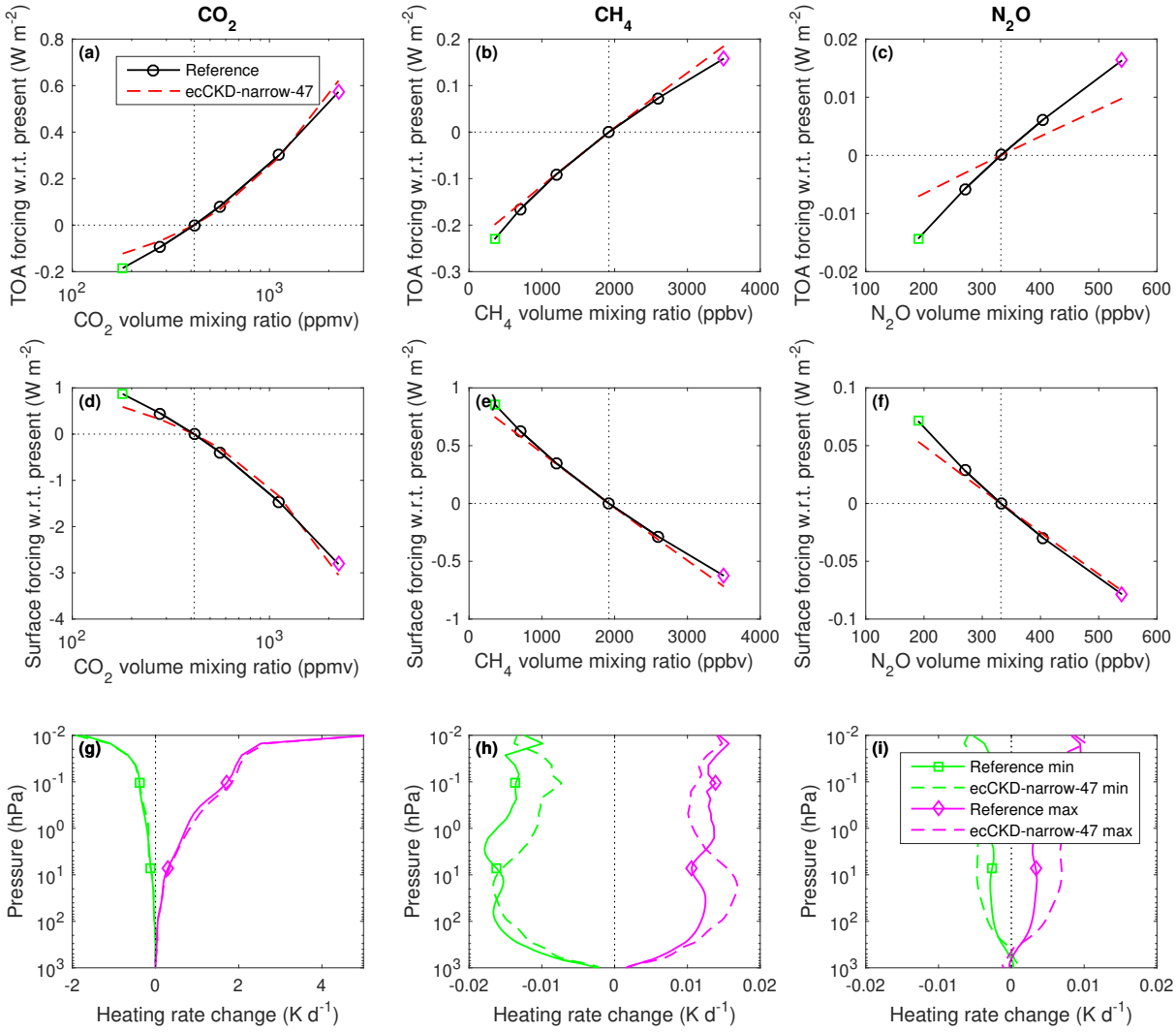

Comparison of reference line-by-line and calculations by the climate-narrow-47 model of the instantaneous clear-sky radiative forcing from perturbing each of the five well-mixed greenhouse gases from their present-day values, at (top row) top-of-atmosphere and (middle row) surface, averaged over the 50 profiles of the Evaluation-1 dataset. The bottom row shows the mean change to heating rate resulting from perturbing the concentration of a gas from its present-day value to either the maximum or minimum value in the range for that gas.

Model 12: ecCKD climate-narrow-66

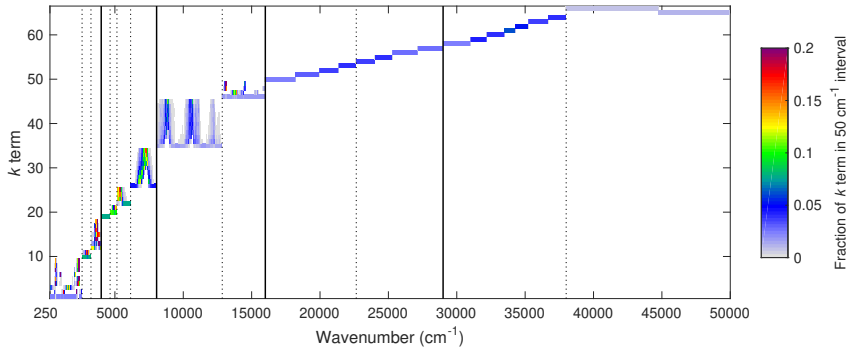

Illustration of the parts of the shortwave spectrum that contribute to each k term of the climate-narrow-66 model.

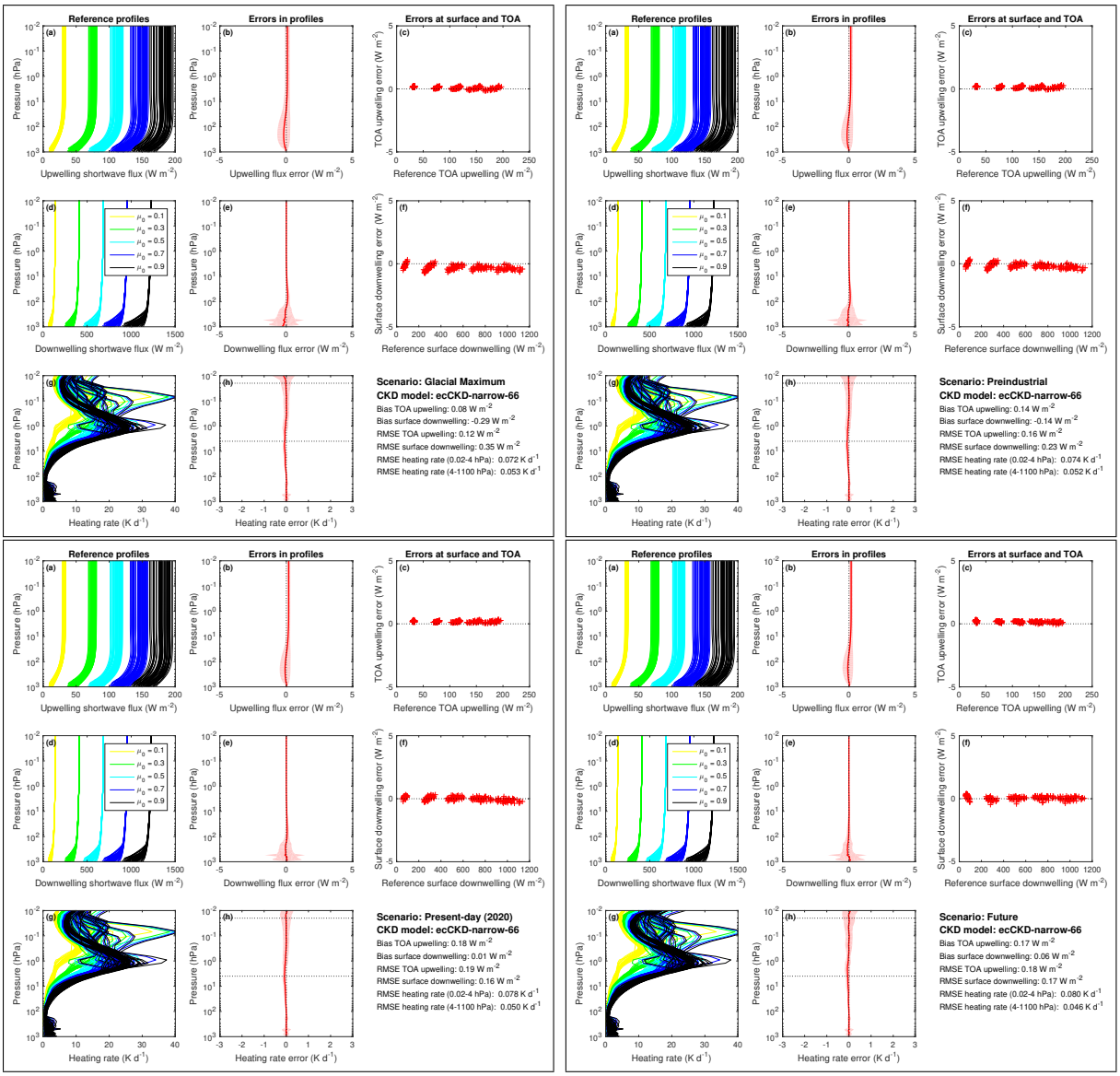

Each boxed group of panels evaluate the climate-narrow-66 CKD model for a single CKDMIP scenario. The left three panels in each group show the irradiances and heating rates from the reference line-by-line calculations for five values of the cosine of the solar zenith angle, μ_0. The red lines in the middle three panels show the corresponding bias in these quantities from the CKD model. The shaded regions encompass 95% of the instantaneous errors. Panels c and f depict instantaneous errors in upwelling TOA and downwelling surface irradiances.

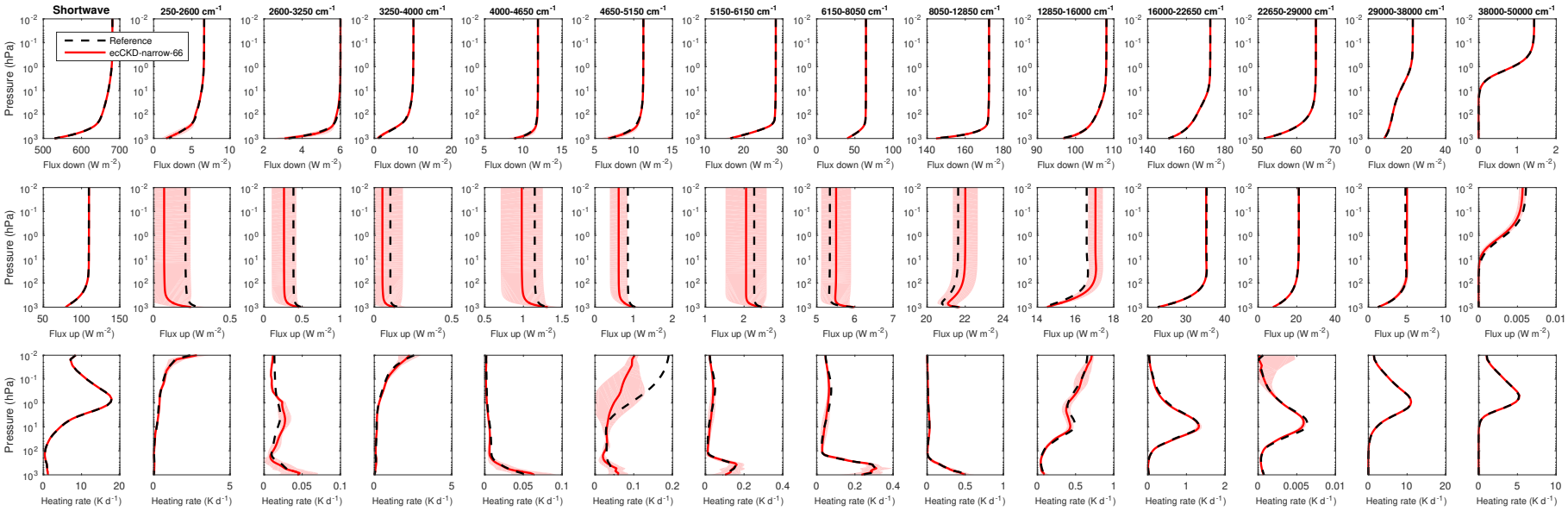

Evaluation of irradiances and heating rates for the broadband (leftmost column of panels) and the 13 narrow shortwave bands (other panels) of the climate-narrow-66 CKD model. The black dashed and red solid lines correspond to the average of the 50 profiles for the "present-day" scenario, while the shaded regions encompass 95% of the error.

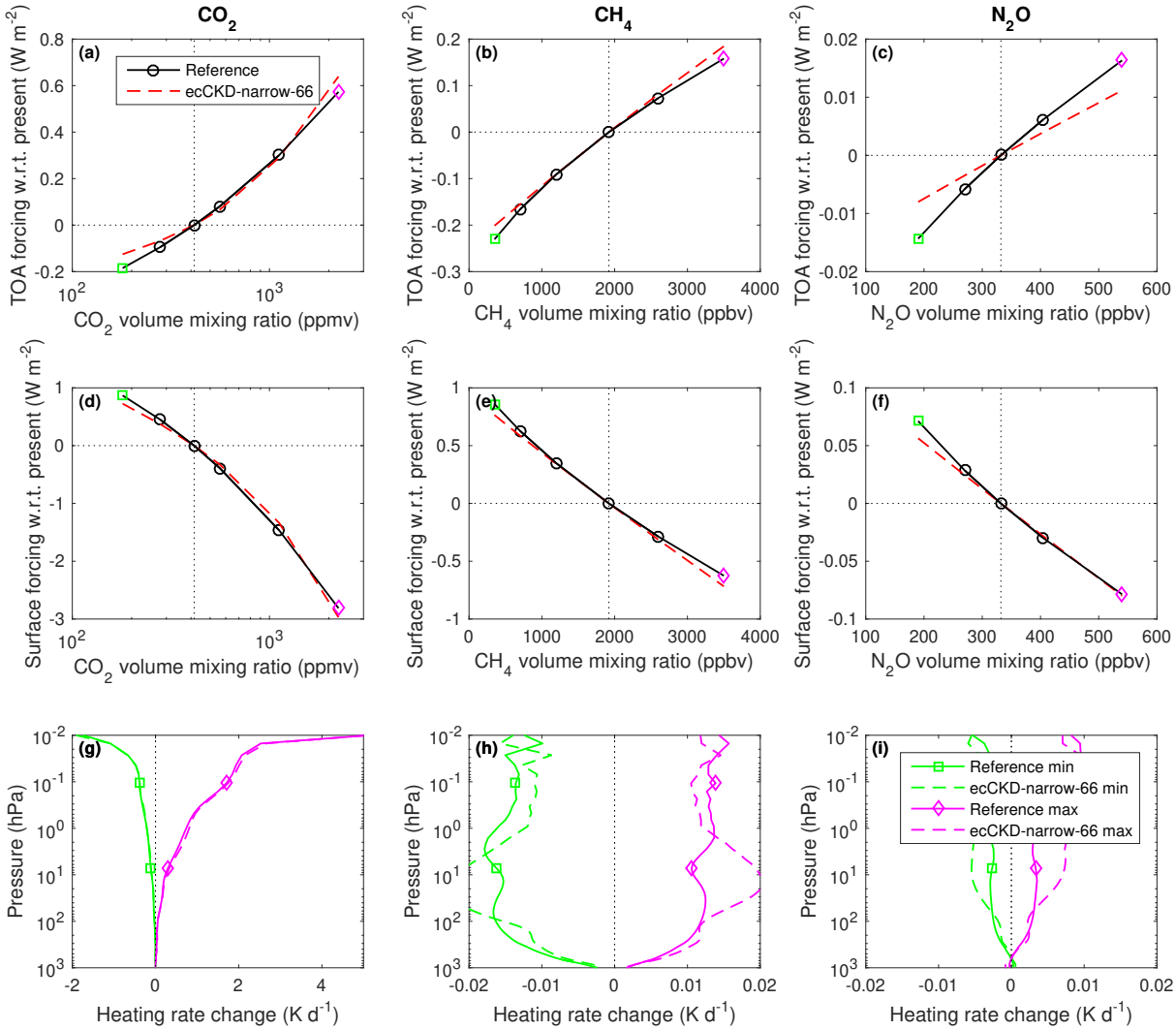

Comparison of reference line-by-line and calculations by the climate-narrow-66 model of the instantaneous clear-sky radiative forcing from perturbing each of the five well-mixed greenhouse gases from their present-day values, at (top row) top-of-atmosphere and (middle row) surface, averaged over the 50 profiles of the Evaluation-1 dataset. The bottom row shows the mean change to heating rate resulting from perturbing the concentration of a gas from its present-day value to either the maximum or minimum value in the range for that gas.